EJN fens European Journal of Neuroscience

European Journal of Neuroscience, Vol. 31, pp. 978–993, 2010 doi:10.1111/j.1460-9568.2010.07133.x

MOLECULAR AND DEVELOPMENTAL NEUROSCIENCE

Biochemical and functional properties of distinct nicotinic acetylcholine receptors in the superior cervical ganglion of mice with targeted deletions of nAChR subunit genes

Reinhard David,[1] Anna Ciuraszkiewicz,[1] Xenia Simeone,[1] Avi Orr-Urtreger,[2] Roger L. Papke,[3] J. M. McIntosh,[4] Sigismund Huck[1] and Petra Scholze[1]

[1]Department of Biochemistry and Molecular Biology, Center for Brain Research, Medical University of Vienna, Spitalgasse 4, A-1090 Vienna, Austria

[2]Genetic Institute, Tel-Aviv Sourasky Medical Center and Sackler School of Medicine, Tel Aviv University, Tel Aviv, Israel

[3]Department of Pharmacology and Therapeutics, University of Florida School of Medicine, Gainesville, FL, USA

[4]Departments of Psychiatry and Biology, University of Utah, Salt Lake City, UT, USA

Keywords: acetylcholine receptor (AChR), immunoprecipitation, knockout, mouse, patch clamp, subunit composition

Abstract

Nicotinic acetylcholine receptors (nAChRs) mediate fast synaptic transmission in ganglia of the autonomic nervous system. Here, we determined the subunit composition of hetero-pentameric nAChRs in the mouse superior cervical ganglion (SCG), the function of distinct receptors (obtained by deletions of nAChR subunit genes) and mechanisms at the level of nAChRs that might compensate for the loss of subunits. As shown by immunoprecipitation and Western blots, wild-type (WT) mice expressed: $\alpha3\beta4$ (55%), $\alpha3\beta4\alpha5$ (24%) and $\alpha3\beta4\beta2$ (21%) nAChRs. nAChRs in $\beta4$ knockout (KO) mice were reduced to < 15% of controls and no longer contained the $\alpha5$ subunit. Compound action potentials, recorded from the postganglionic (internal carotid) nerve and induced by preganglionic nerve stimulation, did not differ between $\alpha5\beta4$ KO and WT mice, suggesting that the reduced number of receptors in the KO mice did not impair transganglionic transmission. Deletions of $\alpha5$ or $\beta2$ did not affect the overall number of receptors and we found no evidence that the two subunits substitute for each other. In addition, dual KOs allowed us to study the functional properties of distinct $\alpha3\beta4$ and $\alpha3\beta2$ receptors that have previously only been investigated in heterologous expression systems. The two receptors strikingly differed in the decay of macroscopic currents, the efficacy of cytisine, and their responses to the α-conotoxins AuIB and MII. Our data, based on biochemical and functional experiments and several mouse KO models, clarify and significantly extend previous observations on the function of nAChRs in heterologous systems and the SCG.

Introduction

In vertebrates, the autonomic nervous system maintains homeostasis under changing physiological demands (De Biasi, 2002). Within ganglia, neurons arising in the brainstem and spinal cord form connections with postganglionic neurons that send their axons to visceral and vascular targets. Mechanisms of ganglionic transmission have been extensively studied in the superior cervical ganglion (SCG), a paravertebral ganglion at the cranial end of the sympathetic chain (Alkadhi *et al.*, 2005a). As the main mediators of fast synaptic transmission in ganglia, neuronal nicotinic acetylcholine receptors (nAChRs) play a key role in ganglionic information processing and transfer (De Biasi, 2002).

nAChRs occur as homo- or hetero-pentamers (McGehee & Role, 1995; Corringer *et al.*, 2000; Brejc *et al.*, 2001). In the SCG, the homo-pentameric receptors are made of the $\alpha7$ subunit, whereas the hetero-pentameric receptors contain the subunits $\alpha3$, $\alpha5$, $\beta2$ and $\beta4$ (Mandelzys *et al.*, 1995; McGehee & Role, 1995; Wang *et al.*, 2002b; Mao *et al.*, 2006; Putz *et al.*, 2008), which might assemble into a variety of receptors of distinct functional properties (McGehee & Role, 1995).

Unfortunately, a great deal of work so far has been done in heterologous expression systems. The disadvantages of such systems include: the effect they might have on the properties of receptors (Lewis *et al.*, 1997), which has led to conflicting observations and also complicates conclusions concerning the nature of native receptors; the absence of chaperones (Millar, 2008); the relative (and sometimes arbitrary) amounts of mRNA used for transfection (Zwart & Vijverberg, 1998); lowered temperature as required when working with *Xenopus* oocytes (Nelson *et al.*, 2003); diversities of N-glycosylation (Sivilotti *et al.*, 1997); and second messengers that may also be involved in the assembling process (Pollock *et al.*, 2009). Cell-specific mechanisms of nAChR expression have recently been summarized in a topical review (Albuquerque *et al.*, 2009).

Correspondence: Dr P. Scholze, as above.
E-mail: Petra.Scholze@meduniwien.ac.at

Received 7 October 2009, revised 28 December 2009, accepted 7 January 2010

The subunit composition and functional properties of nAChRs in dopaminergic neurons have previously been investigated by combining immunoprecipitation, patch clamp, [^{3}H]-dopamine release and mouse knock-out (KO) models (Champtiaux *et al.*, 2003). However, due to the presence of the subunits α4, α5, α6, β2, β3 and β4, nAChRs in dopaminergic neurons show considerable complexity and occur at mixed populations both at somata and at dopaminergic projections (Champtiaux *et al.*, 2003). By taking a similar approach we established the types of hetero-pentameric nAChRs occurring naturally in the wild-type (WT) mouse SCG. Using appropriate KO models we were able to investigate SCG neurons expressing either simple α3β4 or α3β2 receptors, or neurons containing α3β4β2 or α3β4α5, in addition to α3β4 nAChRs. We analysed the functional properties of these receptors, whether a missing subunit would be compensated for at the receptor level and what effect this might have on transganglionic transmission in the SCG.

Methods

Animals and acute preparation of ganglia

Experiments were performed on WT C57Bl/6 mice, and on mice with deletions of the nAChR subunit genes α7 (Orr-Urtreger *et al.*, 1997), α5 (Wang *et al.*, 2002a), β2 (Picciotto *et al.*, 1995), β4 (Kedmi *et al.*, 2004) and α5β4 (Kedmi *et al.*, 2004). β2 KO mice were generously provided by J.-P. Changeux (Pasteur Institute, Paris, France). α7 KO mice were purchased from Jackson Laboratory (Bar Harbor, ME, USA). Double KO mice lacking both α5 and β2 were generated by crossing the two single KO lines. α5α7β2-triple KO mice were obtained by crossing α5β2-double with α7-single KO animals. Mice used in this study were backcrossed onto C57Bl/6 background for six (β4 and α5β4), seven (α5, α7) or 12 (β2) generations after germline transmission. All animals were kept in thermally stable rooms (21°C) on a 10/14-h light–dark schedule in group cages with food and water freely accessible. Animal care and experiments were in accordance with the European Communities Council directive (86/609/EEC) and the Austrian federal law governing animal experimentation (Tierversuchsgesetz TVG 501/1989).

Mice generally 18 days old (P18, range 17–19 days) were deeply anesthetized with CO_2 and killed by decapitation. SCG were collected in Ca^{2+}-free Tyrode's solution: 150 mM NaCl, 4 mM KCl, 2.0 mM $MgCl_2$, 10 mM glucose and 10 mM HEPES (pH 7.4). After removal of the Tyrode's solution, ganglia were flash-frozen with liquid nitrogen and stored at −80°C for later use.

Transganglionic transmission

Adult mice of either sex at the age of 4-6 weeks were put under deep CO_2 anesthesia and decapitated while the heart was still beating. The two SCGs with their pre- and postsynaptic nerves attached were removed and kept in oxygenated Locke's solution for the entire experiment. The composition of the Locke's solution was (mM): NaCl 136, KCl 5.6, $CaCl_2$ 2.2, $MgCl_2$ 1.2, NaH_2PO_4 1.2, $NaHCO_3$ 20 and dextrose 8, continuously bubbled with 95% O_2 and 5% CO_2 (pH 7.2–7.4). Preganglionic nerves were supramaximally stimulated with a suction electrode connected to an ISO-Flex stimulus isolator/Master 8 pulse generator (A.M.P.I., Jerusalem, Israel) at 0.5 Hz with a pulse width of 50 μs. Compound action potentials of the postganglionic (internal carotid) nerve were measured at room temperature with a suction electrode and a differential amplifier (Meta Metrics Corp., Carlisle, MA, USA). The amplitudes of 20 compound action potentials were averaged for a comparison of the three different genotypes: WT, α5β4 KO and α5β2 KO.

Cell culture of SCG neurons

SCGs were dissected from 5- to 6-day-old (P5–P6) mouse pups killed by decapitation. The use of enzymes, the trituration protocol and the culture conditions were similar to published procedures (Fischer *et al.*, 2005), except that 10% fetal calf serum (Sigma F7524) was added to the culture medium for trituration. We seeded 10 000 cells into 8-mm glass rings in order to confine the cells to the center of 35-mm tissue culture dishes (Nunc, Roskilde, Denmark). Cells were routinely cultured at 5% CO_2 and 36.5°C for 3–5 days before use. Unless otherwise stated, cells from α5β4 KO mice were kept in the presence of 100 μM nicotine, added to cultures after 1 day *in vitro* and removed at least 2 h before the recordings.

Membrane preparation

We homogenized tissue (cerebellum, SCG or HEK cells) in ice-cold homogenization buffer [10 mM HEPES, 1 mM EDTA, 300 mM sucrose, pH 7.5, supplemented with one complete mini protease inhibitor cocktail tablet (Roche) per 10 mL buffer]. Exactly three pulses of 5-s duration with the power level set to 30% were delivered by an ultrasonic homogenizer (Bandelin Sonopuls UW2200). We took great care to avoid excessive foam formation by precise positioning of the MS73 sonotrode tip. Following centrifugation of the homogenate for 30 min at 4°C and 50 000 ***g***, the pellet was re-suspended in homogenization buffer without sucrose, incubated on ice for 30 min and centrifuged again for 30 min at 50 000 ***g***. Membrane preparations were always used the same day.

[^{3}H]-epibatidine membrane binding

Membranes prepared as described above were homogenized in 50 mM Tris-HCl (pH 7.4). Membranes of 2–4 SCG (equivalent to 10−20 μg membrane protein) per reaction tube were incubated with [^{3}H]-epibatidine ([5,6.bicycloheptyl-^{3}H](±)epibatidine, NEN-Perkin-Elmer) in a final volume of 200 μL for 2 h at room temperature. Non-specific binding was determined by the presence of 300 μM nicotine and was subtracted from total binding in order to obtain specific binding. Receptors were separated from free ligand by vacuum filtration over GF/B glass-microfiber filters (Whatman, Schleicher & Schuell) that were pre-wet with 0.5% polyethyleneimine (Sigma P3143). Filters were submerged in scintillation cocktail, and their radioactive contents were determined by liquid scintillation counting.

Generation and purification of antibodies

All antibodies were targeted against the cytoplasmic loop region of mouse nAChR subunits: anti-α3 against amino acids 354–467; anti-α4 against amino acids 365–446; anti-α5 against amino acids 333–389; anti-β2 against amino acids 353–422; and anti-β4 against amino acids 350–426. Rabbits were immunized with a maltose binding fusion protein linked to the corresponding loop peptide. The antibodies were purified by using the corresponding glutathione S-transferase fusion protein coupled to Affi-Gel 10 (Bio-Rad).

Immunoprecipitation of [^{3}H]-epibatidine-labeled receptors

Receptors were solubilized by re-suspending membrane preparations (described above) in 2% Triton X-100 lysis buffer: 50 mM Tris-HCl (pH 7.5), 150 mM NaCl, 2% Triton X-100, supplemented with one complete mini protease inhibitor cocktail tablet (Roche) per 10 mL buffer. Following two ultrasound pulses of 5-s duration at 30% energy level, samples were left for 2 h at 4°C and thereafter centrifuged at 16 000 ***g*** for 15 min at 4°C. Then, 150 μL clear supernatant containing the membranes of three SCG (WT, α5 KO, β2 KO, α5β2 KO) or ten SCG (β4 KO, α5β4 KO), respectively, were incubated with 20 μL 10 nM [^{3}H]-epibatidine and 7 μg antibody in 10–15 μL phosphate-buffered saline (PBS: 10 mM Na_2HPO_4, 1.8 mM KH_2PO_4, 2.7 mM KCl, 140 mM NaCl, pH 7.4) on a shaking platform at 4°C overnight. On average, we obtained 1–1.5 μg solubilized protein from our ganglia. Unspecific binding was determined by adding 300 μM nicotine to half of the samples.

Heat-killed, formalin-fixed *Staphylococcus aureus* cells carrying protein A (Standardized Pansorbin-cells, Calbiochem) were centrifuged at 2300 ***g*** for 5 min at 4°C. The pellets were washed twice with IP-High [50 mM Tris–HCl (pH 8.3), 600 mM NaCl, 1 mM EDTA, 0.5% Triton X-100], once in IP-Low [50 mM Tris–HCl (pH 8.0), 150 mM NaCl, 1 mM EDTA, 0.2% Triton X-100] and re-suspended with IP-Low. Then, 20 μL of this suspension of Pansorbin cells was added to the above-mentioned cocktail containing the antibody, solubilized receptors and [^{3}H]-epibatidine for 2 h at 4°C on a shaking platform. Samples were centrifuged at 2300 ***g*** for 5 min at 4°C and washed twice with IP-High and once with IP-Low at 2300 ***g*** for 1 min at 4°C. Pellets were re-suspended in 200 μL 1 N NaOH and subjected to liquid scintillation counting.

Quantification of protein contents in membrane preparations and lysates

All protein quantifications were performed using the Micro BCA Protein Assay Reagent Kit (Pierce, Rockford, IL, USA) following the manufacturer's instructions.

Immunoprecipitation of receptors followed by Western blot

For each sample of lysed receptors, 20 μL M-20 sheep anti-rabbit immunoglobulin G Dynabeads (Invitrogen) were washed three times and re-suspended in 150 μL 2% Triton X-100 lysis buffer. Triton X-100 lysates of SCG membranes were prepared as described above for radioligand immunoprecipitation. Lysates of 15 SCG (corresponding to 15–20 μg lysate protein) were incubated with 150 μL pre-washed Dynabeads and 7 μg antibody on a shaking platform at 4°C overnight. Dynabeads were pelleted using a magnet supplied by the manufacturer, washed three times in 500 μL PBS, re-suspended in 20 μL SDS-PAGE sample buffer and heated to 65°C for 15 min.

SDS-PAGE, Western blot and chemoluminescence detection

Twenty micoliters of tissue lysates was diluted in reducing sample buffer to a final concentration of 62.5 mM Tris/HCl (pH 6.8), 5% α-mercaptoethanol, 2% sodium dodecyl sulfate (SDS), 10% glycerol and 0.01% PyroninY. These samples, or the 20-μL samples released from Dynabeads described above, were denatured for 15 min at 65°C and separated on 10% SDS gels using a Tris-glycine buffer system (25 mM Tris, 192 mM glycine, 0.1% SDS). The size of proteins was determined by mixing 0.3 μL MagicMark XP Western Protein Standard (Invitrogen) with 10 μL SeeBlue Plus2 Pre-Stained Standard (Invitrogen). Proteins were tank-blotted onto pre-wetted polyvinylidene fluoride membranes (Immobilon-P PVDF-Membrane, Millipore IPVH00010). After blocking with blocking buffer (5% non-fat dry milk powder in PBS, 0.1% Tween 20) overnight at 4°C, the membranes were incubated with 1 μg/mL primary antibody in blocking buffer for 2 h at room temperature.

Membranes were then washed extensively with washing buffer (1.5% non-fat dry milk powder in PBS including 0.1% Tween 20) and incubated for 1 h at room temperature with peroxidase-conjugated mouse anti-rabbit light chain-specific secondary antibody (Jackson ImmunoResearch Laboratories), diluted 1 : 10 000 in washing buffer. Following another extensive washing step, membranes were submerged in Immobilon Western Chemiluminescent HRP substrate (Millipore WBKLS0500) for 5 min and sealed in foil. Signals were documented with a Fluor-S Max Multi-Imager (BioRad).

Patch clamp recordings

We used standard techniques for perforated patch clamp recordings as previously described (Fischer *et al.*, 2005). The internal (pipette) solution consisted of 75 mM K_2SO_4, 55 mM KCl, 8.0 mM $MgCl_2$ and 10 mM HEPES, adjusted to pH 7.3 with KOH. Access to cells was achieved by including 200 μg/mL amphotericin B (Rae *et al.*, 1991). Cells were voltage-clamped at −70 mV. For recording and signal processing we used an Axopatch 200B patch clamp amplifier, a Digidata 1320A data acquisition system and pCLAMP 10 software (all from Molecular Devices).

Application of substances

Substances were dissolved in external (bathing) solution consisting of: 120 mM NaCl, 3.0 mM KCl, 2.0 mM $CaCl_2$, 2.0 mM $MgCl_2$, 20 mM glucose, 10 mM HEPES and 0.5 μM tetrodotoxin (TTX, Latoxan), adjusted to pH 7.3 with NaOH. Bovine serum albumin at 0.1 mg/mL was added to solutions when probing the effects of the α-conotoxins AuIB and MII. In order to block muscarinic responses, ACh was always combined with 0.1 μM atropine. The substances were applied by means of a DAD-12 solenoid-controlled superfusion system (ALA Scientific Instruments) with a tip diameter of 100 μm and reservoirs set to a pressure of 250 mmHg. With the tip of the superfusion placed 120 μm above our cells we reach 75% of the final concentration of solutions within 35 ms. This is considerably slower than the rapid application system used by others (full concentration reached within 5 ms) to record the currents carried by the fast desensitizing splice variant α7-1 of the α7 nAChR (Zhang *et al.*, 1994; Severance *et al.*, 2004). By comparing their rapid application with a conventional but slower puffer pipette, these authors concluded that the high speed of the superfusion is a prerequisite for the detection of currents in response to α7-1 activation in chick ciliary ganglion neurons (Zhang *et al.*, 1994). Upon probing our DAD-12 superfusion set-up on freshly dissociated embryonic day 14 (E14) chick ciliary ganglion neurons we recorded rapidly decaying α7-1 currents (see Supporting information, Fig. S2), but of a lesser amplitude than has been reported (Zhang *et al.*, 1994). Although response kinetics of α7-1 receptors are most affected, the limited speed of our superfusion system will also just partly disclose the quality of α3β2 receptor activation. Relatively slowly desensitizing receptors such as α3β4 will be least affected.

Reagents

General chemical reagents were from Merck-VWR-Jencons. Substances not particularly mentioned were from Sigma-Aldrich. PNU-120596 (# 2498) and cytisine (# 1390) were from Tocris.

Data analysis

Unless indicated otherwise, all data are presented as means ± SEM. Statistical analyses and curve fitting were done with GRAPHPAD PRISM version 4.0 (GraphPad Software). Data points for the binding of [^{3}H]-epibatidine were fitted to a hyperbolic curve based on a one-site model. Concentration–response measurements of drug effects were fitted to sigmoidal curves using the logistic equation:

$$E_{(x)} = E_{\max} \times x^p / (x^p + \mathrm{EC}_{50})$$

where $E_{(x)}$ is the response to a certain drug concentration, x is the arithmetic dose, $E_{\max}$ is the maximal response, EC_{50} is the dose that gives half-maximal response and p is a slope factor, which is numerically identical to the Hill coefficient. Agonist low-concentration potency ratios were calculated as previously described (Fischer *et al.*, 2005), except that we now use the curve fitting routine of GraphPad Prism with the constraints of a shared slope and with maximal responses fixed to values deduced from parallel experiments. Student's *t*-test, one-way analysis of variance (ANOVA), or non-parametric Mann–Whitney or Wilcoxon tests were performed when appropriate. The decay of currents in the presence of an agonist was fitted to two standard exponentials curves using the Chebyshev algorithm included in the CLAMPFIT software (Molecular Devices).

Results

Membrane binding of [^{3}H]-epibatidine to nicotinic receptors is significantly reduced in the SCG of β4 KO mice

We first determined the kinetics of [^{3}H]-epibatidine binding to SCG membrane homogenates of 17- to 19-day-old (mostly P18) WT mice. Binding was saturable with a dissociation constant (K_D) of 150.7 ± 25.6 pM and a maximum binding capacity (B_{max}) 345.8 ± 25.6 fmol/mg protein (Fig. 1A; $n = 4$ different experiments). Binding was maximal at 1 nM epibatidine, the concentration used thereafter for all further assessments of the total number of hetero-oligomeric nAChR binding sites. Epibatidine binds with high affinity in the picomolar range to hetero-oligomeric nAChRs (Houghtling *et al.*, 1995), and with much lower affinity (greatly in excess to 1 nM) to α7 homo-oligomeric nAChRs (Sharples *et al.*, 2000). In keeping with these reports we did not find significantly reduced [^{3}H]-epibatidine binding when using SCG membranes from α5α7β2 KO mice (Fig. 1B).

Figure 1B compares the specific [^{3}H]-epibatidine binding in membrane homogenates prepared from SCGs of WT and six different KO mouse lines. Note that the number of receptors was significantly reduced not only in α5β4-double, but also in β4-single KO mice (to 8 and 13% of control, respectively, Fig. 1B). None of the other genotypes, including the α5α7β2-triple KO, showed a reduced number of [^{3}H]-epibatidine binding sites (genotypes compared by one-way ANOVA, $F = 35.46$, $P < 0.0001$, followed by Dunnett's *post-hoc* multiple comparison test referenced to wild-type, $^{**}P < 0.01$ for β4-single and α5β4-double KO, all other $P > 0.05$).

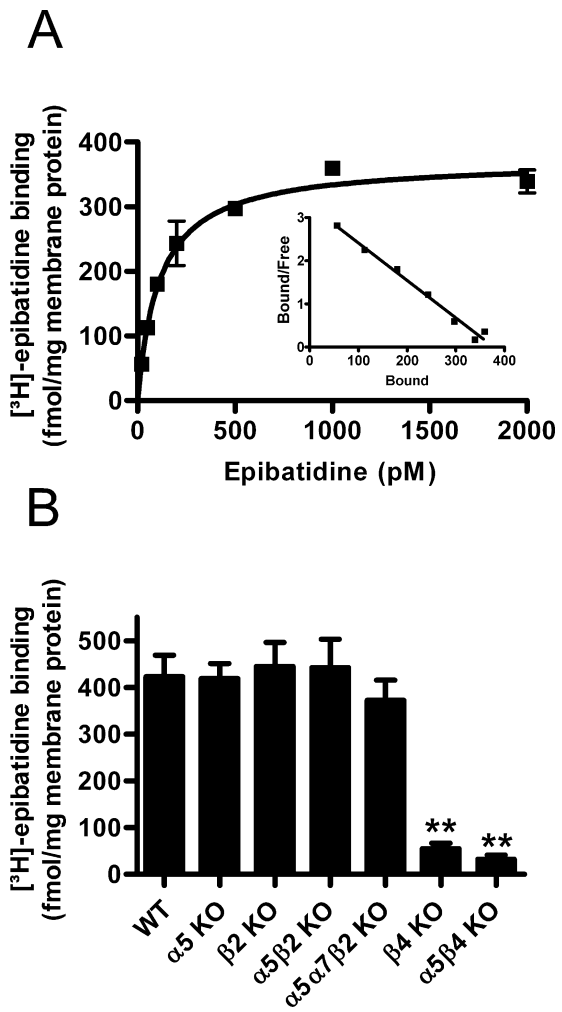

FIG. 1. [^{3}H]-epibatidine binding sites are significantly reduced in α5β4-double and β4-single KO mice. (A) Kinetics of [^{3}H]-epibatidine binding to membrane homogenates from WT mouse SCG. Data points are means of specific binding ± SEM of duplicate measurements. Non-specific binding determined by the presence of 300 μM nicotine was subtracted from overall to obtain specific binding. Parameters of the curve fitted to the data points were 112.6 ± 9.1 pM (K_D) and 371.2 ± 13.5 fmol/mg protein (B_{max}). Inset: Scatchard plot of data [abscissa: bound [^{3}H]-epibatidine (fmol/mg); ordinate: bound/free [^{3}H]-epibatidine (fmol/mg protein)/pM)]. Averaged kinetic parameters ± SEM from four such experiments were 150.7 ± 25.6 pM (K_D) and 345.8 ± 25.6 fmol/mg protein (B_{max}). (B) Specific binding of 1 nM [^{3}H]-epibatidine to SCG membrane homogenates taken from WT mice and from mice with distinct deletions of indicated nAChR subunit genes. Data are means ± SEM of 3–10 independent experiments, each performed with triplicate measurements. Compared with WT SCG, [^{3}H]-epibatidine binding was significantly reduced only in α5β4-double and β4-single KO animals (one-way ANOVA, $F = 35.46$, $P < 0.0001$, followed by Dunnett's *post-hoc* test, $^{**}P < 0.01$). [^{3}H]-epibatidine binding sites did not differ significantly between α5β4-double (7.8% of WT) and β4-single KO animals (13.2% of WT, Student's *t*-test).

Antibodies for immunoprecipitation assays

Subunit-specific antibodies are essential prerequisites for the analysis of the subunit composition of nAChR subtypes. We thus generated antibodies directed against the subunits α3, α4, α5, β2 and β4. With the exception of anti-α3, all antibodies were tested not only on native receptors of WT mice (positive controls) but also on neuronal materials of appropriate KO animals (negative controls). Such rigorous controls are essential to exclude false-positive results (Gotti *et al.*, 2006; Moser *et al.*, 2007). A detailed characterization of these antibodies is provided in the supporting Fig. S1. Note that our antibodies are not only highly specific but also immunoprecipitate

with excellent efficacy, as shown by comparison with polyethyleneglycol precipitation (supporting Fig. S1). Polyethyleneglycol precipitates all proteins in solution and thus serves as a reference for 100% of precipitated, radioligand-labeled receptors.

Each neuronal-type hetero-oligomeric receptor must contain either $\beta2$ and/or a $\beta4$ (Champtiaux & Changeux, 2004). We judged the overall number of [^{3}H]-epibatidine binding sites by immunoprecipitation with anti-$\beta2$ and anti-$\beta4$ antibodies used in conjunction, and deduced the relative occurrence of receptors made of the subunits $\alpha3$, $\alpha4$, $\alpha5$, $\beta2$ and $\beta4$ by precipitations with appropriate subunit-specific antibodies in isolation. However, the use of either anti-$\beta4$ or anti-$\beta2$ in $\beta2$ and $\beta4$ KO animals, respectively, will suffice to immunoprecipitate all hetero-oligomeric receptors in the SCG of these mice. Anti-$\alpha3$ antibodies consistently immunoprecipitated the same number of receptors as either anti-$\beta4$, anti-$\beta2$ (in their complementary KO) or the combined use of the two antibodies (Fig. 2), indicating that all receptors in the SCG of P18 mice contain $\alpha3$. It is worth noting that $\alpha4$-containing receptors are absent in the SCG not only of P18 mice (Fig. 2A–D) but also of adult rats (Mao *et al.*, 2006).

Receptors containing the accessory subunits $\alpha5$ and $\beta2$

As shown in Fig. 2A, 100% of receptors in the SCG of WT animals contain the subunits $\alpha3$ and $\beta4$. Anti-$\alpha5$ as well as anti-$\beta2$ antibodies precipitated approximately 20% of all receptors. These observations allow, in principle, for four types of receptors: $\alpha3\beta4$, $\alpha3\beta4\alpha5$, $\alpha3\beta4\beta2$ and $\alpha3\beta4\alpha5\beta2$. To investigate whether all these combinations are present in the mouse SCG we immunoprecipitated receptors using the anti-$\alpha5$ and anti-$\beta2$ antibodies alone and in combination (Fig. 3C). The algebraic sum (429 ± 93 fmol/mg protein) did not differ significantly from results when the two antibodies were used together (402 ± 98 fmol/mg protein; $P > 0.05$; one-way ANOVA, followed by Dunnett's *post-hoc* multiple comparison test referenced to the combined use of both antibodies). In contrast, each antibody alone (anti-$\alpha5$: 250 ± 79 fmol [^{3}H]-epibatidine per mg protein; anti-$\beta2$: 179 ± 15 fmol/mg protein) precipitated significantly less [^{3}H]-epibatidine receptor binding sites than the combination of both antibodies (**$P < 0.01$; one-way ANOVA, followed by Dunnett's *post-hoc* multiple comparison test referenced to the combined use of both antibodies). These data suggest that $\alpha5$ and $\beta2$ are not co-expressed in the same receptor, and that only three types of receptors are present in the SCG of P18 WT mice: $\alpha3\beta4$ (55%), $\alpha3\beta4\alpha5$ (24%) and $\alpha3\beta4\beta2$ (21%, Fig. 2A).

Further evidence that $\alpha5$ does not co-assemble with $\beta2$

Western blots provided further evidence that $\alpha5$ does not co-assemble into the same receptor with $\beta2$. Hence, immunoprecipitation with anti-$\alpha3$, but not with anti-$\alpha5$, resulted in a band of approximately 52 kDa

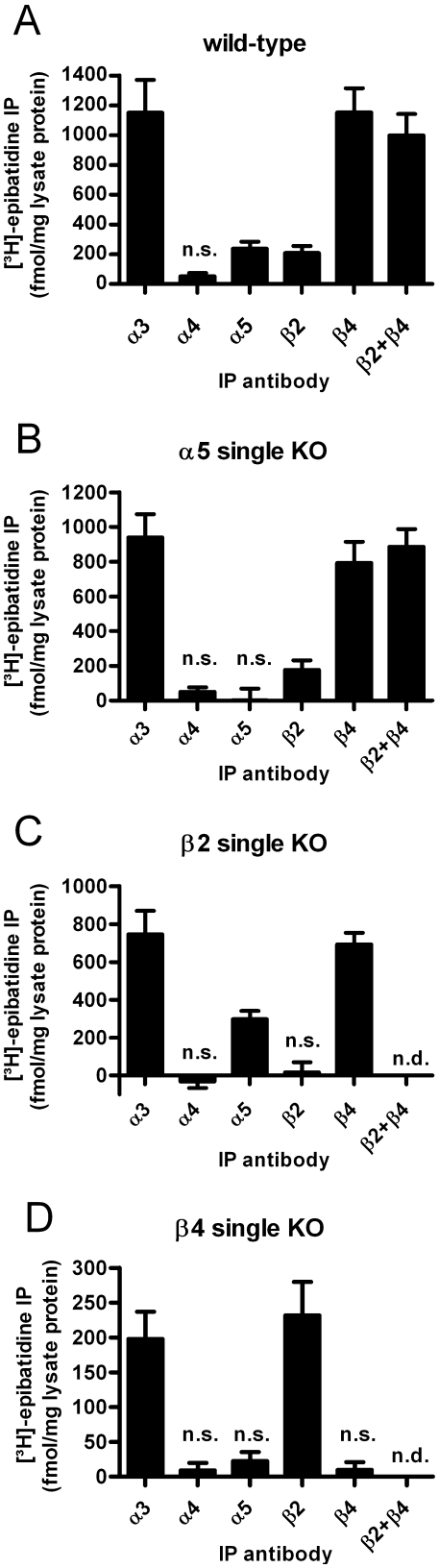

FIG. 2. Subunit composition of nAChRs in the wild-type mouse SCG, and absence of compensation in the SCG of mice with deletions of a single nAChR subunit gene. nAChRs from SCG membranes of wild-type mice (A) or mice with deletions of the $\alpha5$ (B), the $\beta2$ (C) or the $\beta4$ subunits (D) were solubilized, labeled with 1 nM [^{3}H]-epibatidine and immunoprecipitated with each of the subunit-specific antibodies indicated at the abscissa. Non-specific binding was measured in the presence of 300 μM nicotine and subtracted from overall to obtain the specific binding shown. Data are means ± SEM of 4–8 independent experiments, each performed in triplicate (A, B and C) or duplicate (D). Note in A and B that anti-$\alpha3$ and anti-$\beta4$ antibodies precipitate an identical number of receptors, and that the combined use of anti-$\beta4$ and anti-$\beta2$ antibodies does not precipitate more receptors than the single use of anti-$\beta4$ antibodies. Levels of $\alpha4$ are not significantly different from zero ($P = 0.052$ in A and $P = 0.189$ in B, one-sample Student's *t*-test). Anti-$\alpha5$ and anti-$\beta2$ antibodies precipitated 24 and 21%, respectively, of the receptors that were precipitated by the combined use of anti-$\beta4$ and anti-$\beta2$ measurements. n.s.: not significantly different from zero ($P > 0.05$, one-sample Student's *t*-test). n.d.: not determined.

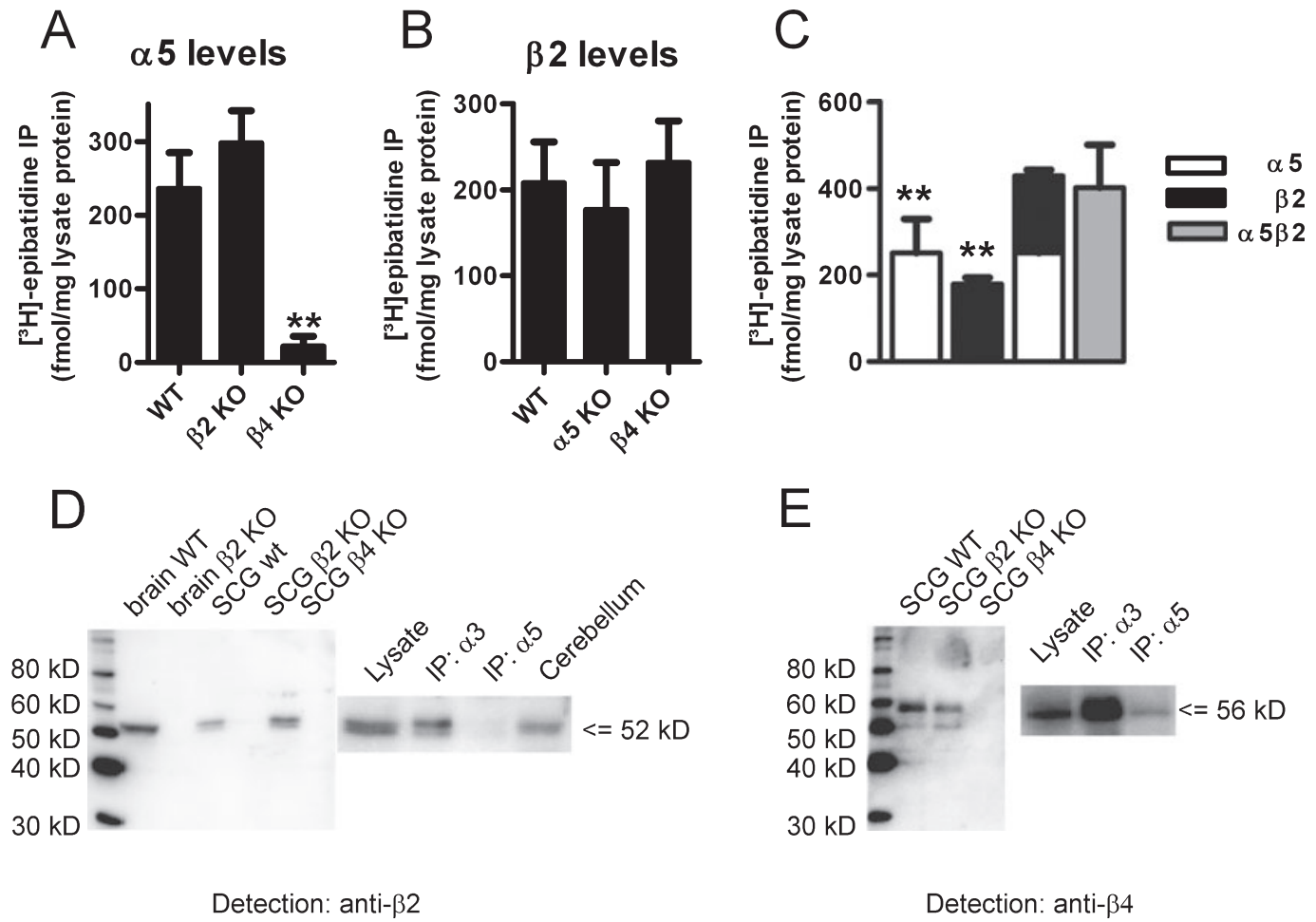

FIG. 3. Subunit composition of nAChRs in the mouse SCG. (A) The α5 subunit co-assembles with *β*4 only and is not up-regulated in the SCG of *β*2 KO mice. nAChRs from SCG membranes of WT, *β*2 and *β*4 KO mice (indicated at the abscissa) were solubilized, labeled with 1 nM [^{3}H]-epibatidine, and immunoprecipitated with our anti-α5 antibody. Data are the mean specific binding ± SEM of 3–8 independent experiments, each performed in triplicate. Note that levels of the α5 subunit do not significantly differ between WT and *β*2 KO animals. In contrast, α5 is lost in the SCG of *β*4 KO mice (not significantly different from zero, $P > 0.05$, one sample Student's *t*-test). All columns were compared using one-way ANOVA, $F = 10.38$, $P = 0.0008$, followed by a Dunnett's *post-hoc* multiple comparison test: WT vs. *β*2 KO: $P > 0.05$; WT vs. *β*4 KO: $^{**}P < 0.01$. (B) The *β*2 subunit does not compensate for the absence of either α5 or *β*4. nAChRs solubilized and labeled as described above were immunoprecipitated with our anti-*β*2 antibody. Data are the mean specific binding ± SEM of 4–6 independent experiments, each performed in triplicate. Note that *β*2 levels do not differ significantly between the three genotypes indicated at the abscissa (one-way ANOVA, $F = 0.227$, $P = 0.800$). (C) The subunits α5 and *β*2 do not co-assemble in the same receptor. nAChRs solubilized and labeled as described above were immunoprecipitated in parallel with anti-α5 (white bars), anti-*β*2 (black bars) or a combination of both antibodies (gray bar). Data are the mean specific binding ± SEM of five independent experiments, each performed in triplicate. The number of receptors immunoprecipitated by each of the single antibodies differed significantly from the number of receptors precipitated by a combination of the two antibodies ($^{**}P < 0.01$). The arithmetic sum of the two individual precipitations is not significantly different from the result obtained by combined immunoprecipitation with both antibodies (repeated-measures one-way ANOVA $F = 14.72$, $P = 0.0003$, followed by a Dunnett's multiple comparison test with data referenced to the result obtained by the combined immunoprecipitation with both antibodies). (D) The α5 subunit does not co-assemble with *β*2. The left part of the figure illustrates the specificity of our anti-*β*2 antibody for Western blot analyses. Note bands of approximately 52 kDa in brain and SCG samples from WT and *β*4 KO animals, and the absence of such bands in *β*2 KO mice. As shown on the right part of the figure, the band can also be detected in Western blots of receptors immunoprecipitated with anti-α3, but not with anti-α5 antibodies. The cerebellum is added as a further positive control. E. The α5 subunit co-assembles with *β*4. The left part of the figure shows the specificity of our anti-*β*4 antibody for Western blot analyses. Note a major band of approximately 56 kDa in SCG samples from WT and *β*2 KO mice and the absence of such a band in *β*4 KO animals. The anti-*β*4 antibody detects a solid band in Western blots of receptors immunoprecipitated with anti-α3, and a much weaker band if receptors were immunoprecipitated with anti-α5 antibodies (right part of the figure).

when probed with our anti-*β*2 antibody (Fig. 3D). Importantly, the anti-*β*2 antibody showed no signal in Western blots from whole-brain or SCG extracts of *β*2 KO animals (Fig. 3D). In contrast, our anti-*β*4 antibody detected a band of approximately 56 kDa when solubilized receptors were immunoprecipitated with either anti-α3 or anti-α5 antibodies (Fig. 3E). These observations provide good evidence that α5 co-assembles with the *β*4 but not with the *β*2 subunit in the SCG of WT animals. Furthermore, α5 could not be forced into co-assembling with *β*2 in our *β*4-single KO mouse model (Figs 2D and 3A). Hence, only a single type of α3*β*2 hetero-oligomeric receptors was found in the SCG not only in α5*β*4-double (supporting Fig. S1), but also in *β*4-single KO mice (Fig. 2D).

The subunits α5 and β2 are tightly regulated in the SCG

Deletion of the α5 subunit did not affect the number of *β*2-containing receptors (Fig. 3B), indicating that *β*2 subunits otherwise unused do not take the place of α5 (in this case the proportion of *β*2-containing receptors should rise from about 20 to 40%). In fact, the number of *β*2-containing receptors remained stable even when the *β*4 subunit

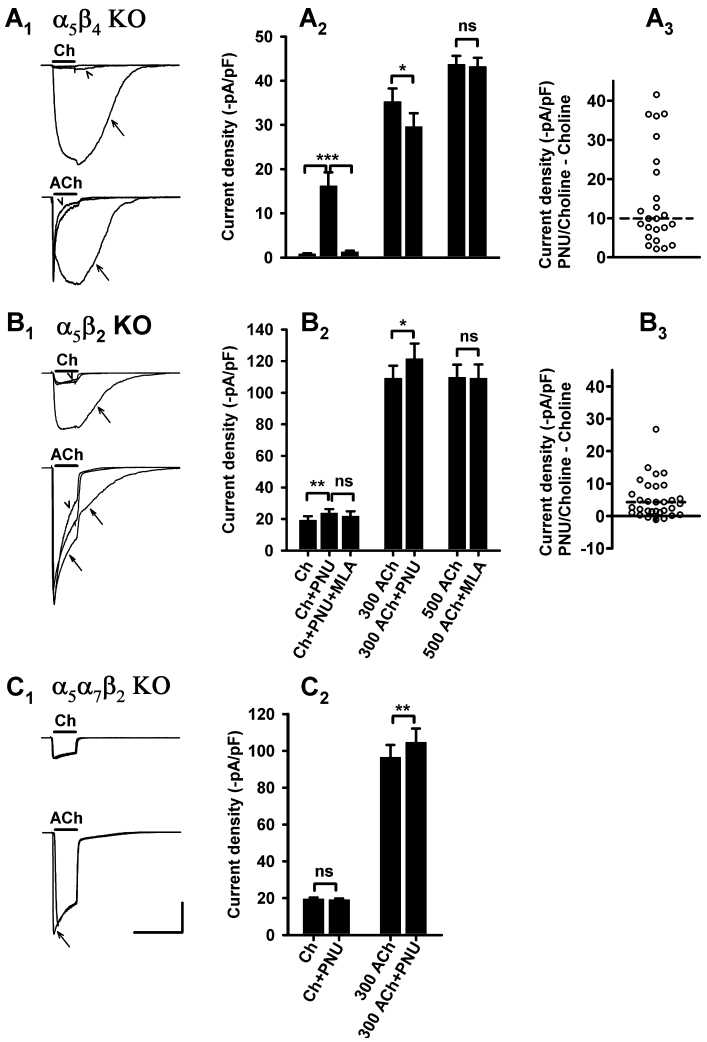

FIG. 4. Probing α7 nAChRs. (A) Patch clamp measurements of SCG neurons from α5β4 KO animals. (A1, upper panel) Unveiling of α7-mediated currents by the type II-positive allosteric modulator PNU-120596, and rapid reversal of the effect by methyllycaconitine (MLA). The figure shows a particularly large effect of PNU-120596. Three superimposed current traces in response to 10 mM choline (Ch, indicated by bar); 10 mM choline in the presence of – and following a 10-s superfusion with – 10 μM PNU-120596 (arrow); pretreatment with 5 nM MLA for 2 min, followed by 10 mM choline plus 10 μM PNU-120596 (arrowhead). Note that choline by itself has a negligible effect. Calibration: 4 s, 1 nA. (A1, lower panel) Same cell, with currents induced by 300 μM ACh (in the presence of 0.1 μM atropine, bar). 10 μM PNU-120596 (arrow) has no effect on initial peak current but gives rise to a large second peak of delayed onset (arrow). Arrowhead denotes current following pretreatment with MLA. Calibration: 4 s, 1 nA. (A2) See panel B2 for a labeling of bars. Choline-induced currents in the presence of 10 μM PNU-120596 (Ch + PNU) are significantly larger than in the absence of PNU (Ch) or after 2 min pretreatment with 5 nM MLA (Ch + PNU + MLA). Paired observations of 18 neurons (***P = 0.0002, Wilcoxon test). Peak currents in response to 300 μM ACh are reduced (*P = 0.0315, paired Student's t-test, n = 13 neurons) in the presence of 10 μM PNU-120596 (300 ACh + PNU). Peak currents in response to 500 μM ACh are unaffected by 2 min pretreatment with 5 nM MLA (500 ACh + MLA) (n = 22 neurons, P = 0.6041, paired Student's t-test). (A3) Net effect of 10 μM PNU-120596 obtained by subtracting the peak current in response to 10 mM choline from choline-induced current in the presence of PNU-120596. Dashed line indicates a median value of 9.90 pA/pF (n = 24 cells). (B) Patch clamp measurements of SCG neurons from α5β2 KO animals. (B1, upper panel) Unveiling of α7-mediated currents by PNU-120596, and rapid reversal of the effect by MLA. The figure shows a particularly large effect of PNU-120596. Three superimposed current traces in response to 10 mM choline (Ch, indicated by bar); 10 mM choline in the presence of – and following a 10-s superfusion with – 10 μM PNU-120596 (arrow); pretreatment with 5 nM MLA for 2 min, followed by 10 mM choline plus 10 μM PNU-120596 (arrowhead). Note that choline by itself has a noticeable effect by activating α3β4 nAChRs. Calibration: 4 s, 2 nA. (B1, lower panel) Same cell, with currents induced by 300 μM ACh (in the presence of 0.1 μM atropine, bar). 10 μM PNU-120596 (arrows) has no effect on initial peak current but slows the decay of the current and the washout. Arrowhead denotes current following pretreatment with MLA. Calibration: 4 s, 2 nA. (B2) Choline-induced currents in the presence of 10 μM PNU-120596 (Ch + PNU) are significantly larger than in the absence of PNU (Ch). Paired observations of 16 neurons (**P = 0.0015, Wilcoxon test). The inhibition of currents in response to choline plus PNU-120596 (Ch + PNU) by 2 min pretreatment with 5 nM MLA (Ch + PNU + MLA) is not statistically significant (P = 0.4156, Wilcoxon test, n = 16). Peak currents in response to 300 μM ACh are enhanced in the presence of 10 μM PNU-120596 (300 ACh + PNU); n = 14 neurons (*P = 0.0163, paired Student's t-test). Peak currents in response to 500 μM ACh are unaffected by 2 min pretreatment with 5 nM MLA (500 ACh + MLA); n = 25 neurons (P = 0.9692, paired Student's t-test). (B3) Net effect of 10 μM PNU-120596 obtained by subtracting the peak current in response to 10 mM choline from choline-induced current in the presence of PNU-120596. Dashed line indicates a median value of 4.29 pA/pF (n = 33 cells). These data differ significantly from the data shown in A3 (P = 0.0023, Mann–Whitney test). (C) Patch clamp measurements of SCG neurons from α5α7β2 KO animals. (C1, upper panel) Currents in response to 10 mM choline (bar) are unaffected by 10 μM PNU-120596. Graph shows two superimposed current traces. The schedule of substance application is identical to panels A1 and B1. Calibration: 4 s, 2 nA. (C1, lower panel) Same cell, with currents induced by 300 μM ACh (in the presence of 0.1 μM atropine, bar). 10 μM PNU-120596 (arrow) has no effect on the time course of receptor desensitization and the washout of ACh. Calibration: 4 s, 2 nA. (C2) Choline-induced currents in the presence of 10 μM PNU-120596 (Ch + PNU) are not significantly different from currents in the absence of PNU (Ch). Paired observations of 35 neurons (P = 0.1918, Wilcoxon test). Peak currents in response to 300 μM ACh are enhanced in the presence of 10 μM PNU-120596 (300 ACh + PNU); n = 26 neurons (**P = 0.0026, paired Student's t-test).

was deleted (Fig. 3B). Because only about 20% of receptors in the SCG of WT animals contain the β2 subunit, this caused a major reduction in the overall number of [^{3}H]-epibatidine receptor binding sites (Figs 1B and 2D).

We also found the α5 subunit is tightly regulated. When comparing WT and β2 KO animals we saw no significant difference in the number of α5-containing receptors, indicating that α5 does not substitute for the loss of β2 (Fig. 3A).

Functional α7 receptors in SCG cell cultures

Once we had established the types of receptors encountered in the SCG, we characterized them functionally by patch clamp recordings. We focused on two hetero-oligomeric receptors consisting of the subunits $\alpha3\beta2$ and $\alpha3\beta4$, as the properties of such 'pure' receptors have so far only been investigated in heterologous expression systems.

To exclude contributions from α7 homo-oligomeric nAChRs we followed published protocols that detect currents due to the activation of α7. SCG neurons freshly dissociated from 10- to 14-day-old rats have two types of currents in response to the activation of two splicing variants of the α7 gene: one of quite low amplitude (α7-1, currents in the pA range) with extremely rapid desensitization kinetics, and a second (α7-2, currents in the nA range) with relatively slow desensitization kinetics (Cuevas *et al.*, 2000; Severance *et al.*, 2004). Currents due to α7-2 activation by 500 μM ACh are inhibited in a reversible manner by both α-bungarotoxin and methyllycaconitine (MLA) (Cuevas *et al.*, 2000). We did not see any inhibition of these currents by MLA (Sigma M168), suggesting that this component, if present in the P5–P7 mouse SCG, is lost when cells are maintained in culture (Fig. 4A$_2$ and B$_2$).

We also probed our cultures for rapidly desensitizing α7 receptors with choline, a full agonist for α7 receptors (Papke *et al.*, 1996; Cuevas *et al.*, 2000). Choline concentrations ranging from 3 to 30 mM induced negligible currents in cultured SCG neurons obtained from $\alpha5\beta4$ KO animals (Fig. 4A$_1$ and A$_2$), but slowly decaying currents of considerable amplitude in our $\alpha5\beta2$ KO preparations (Fig. 4B$_1$ and B$_2$). The slowly desensitizing currents were due to the sole activation of $\alpha3\beta4$ without any contribution by α7 receptors, as they were also seen in our $\alpha5\alpha7\beta2$-triple KO mice (Fig. 4C$_1$ and C$_2$).

We never experienced a rapidly decaying component as seen in freshly dissociated rat SCG neurons (Cuevas *et al.*, 2000). However, choline effects were boosted to a variable extent by the positive allosteric α7 modulator PNU-120596 (Hurst *et al.*, 2005), and this effect was reversed by 2 min pre-treatment with 5 nM MLA (Fig. 4). Because $\alpha3\beta2$ receptors were hardly activated by choline, the effects of PNU-120596 were more obvious in SCG neurons of $\alpha5\beta4$ than of $\alpha5\beta2$ KO mice (Fig. 4, compare A$_2$ with B$_2$). Nonetheless, net PNU-120596 effects (seen by subtracting peak currents in the absence of the α7 modulator from currents in the presence of PNU-120596) were significantly larger in $\alpha5\beta2$ KO than in $\alpha5\beta4$ KO animals ($P = 0.0023$, Mann–Whitney comparison of data shown in Fig. 4A$_3$ and B$_3$). PNU-120596 had no effect in the absence of choline, nor did it enhance choline-induced currents in $\alpha5\alpha7\beta2$-triple KO mice subunit (Fig. 4C$_1$ and C$_2$), indicating that the effect of the modulator is indeed specific for α7. The small enhancement of ACh-induced currents by PNU-120596 in $\alpha5\beta2$ KO animals (Fig. 4B$_2$) seems unrelated to an effect on α7 receptors, as it is also seen in our $\alpha5\alpha7\beta2$-triple KO mice (Fig. 4C$_2$).

We also tested 10 μM PNU-120596 on freshly dissociated E14 chick ciliary ganglion neurons, a preparation renowned for its high density of rapidly inactivating α7 receptors (Zhang *et al.*, 1994). Peak currents in response to 10 mM choline (40.4 ± 3.8 pA/pF, $n = 15$) increased to 1688 ± 204 pA/pF in the presence of PNU-120596 (supporting Fig. S2). In view of this observation, the effect of PNU-120596 in cultured SCG neurons appears unimpressive (median values of 4.29 and 9.90 pA/pF for $\alpha5\beta2$ and $\alpha5\beta4$ KO, respectively; Fig. 4A$_3$ and B$_3$). We thus conclude that functional α7-1 receptors are expressed in cultured mouse SCG neurons, but due to their small size are detected by our techniques only in the presence of PNU-120596. It is worth noting that rapidly desensitizing currents due to α7-1 in freshly dissociated rat SCG neurons are significantly smaller (currents in the pA range, Cuevas *et al.*, 2000) than in chick ciliary ganglion neurons (currents in the nA range, Zhang *et al.*, 1994) and thus are much more likely to be missed. Previous attempts to record α-bungarotoxin-sensitive currents in cultured rat SCG neurons have equally failed, in spite of clear [^{125}I]-α-bungarotoxin binding to plasma membrane receptors in intact neurons (De Koninck & Cooper, 1995).

$\alpha3\beta2$ receptors in the mouse SCG

In the absence of measurable α7 responses, the currents remaining in our $\alpha5\beta4$-double KO mice will be due to just $\alpha3\beta2$ receptor activation. Agonist-induced peak currents in cultured SCG neurons taken from $\alpha5\beta4$ KO mice were significantly smaller than from $\alpha5\beta2$ KO animals (Tables 1 and 2, compare Figs 5 and 6). These results are in keeping with our observation of a reduced number of [^{3}H]-epibatidine binding sites in the SCGs of P18 $\alpha5\beta4$ KO animals (Fig. 1B) and suggest that not only is the total number of receptors reduced in animals lacking the β4 subunit but so too is the number of plasma membrane receptors. Culturing neurons from $\alpha5\beta4$ KO animals in the presence of 100 μM nicotine increased the currents in response to ACh (Fig. 5C), although

TABLE 1. Pharmacological properties of distinct nAChRs

nAChRs and agonists	EC50	Hill coefficient	Max current density (−pA/pF)
(A) $\alpha3\beta4$ receptors (in $\alpha5\beta2$ KO)			
DMPP ($n = 26$)	19.04 ± 0.76	1.91 ± 0.06	107.8 ± 6.7*
Cytisine ($n = 24$)	34.5 ± 2.26	1.44 ± 0.06	124.5 ± 9.2*
Nicotine ($n = 25$)	32.95 ± 1.34	1.68 ± 0.06	115.6 ± 7.9*
ACh ($n = 24$)	101.4 ± 4.65	1.60 ± 0.05	134.79 ± 11.2*
(B) $\alpha3\beta4\alpha5$ receptors (in $\beta2$ KO)			
DMPP ($n = 26$)	23.03 ± 1.17	1.79 ± 0.08	91.73 ± 6.30†
Cytisine ($n = 26$)	37.69 ± 2.43	1.10 ± 0.02	121.12 ± 8.02†
Nicotine ($n = 0$)	n.d.	n.d.	n.d.
ACh ($n = 0$)	n.d.	n.d.	n.d.
(C) $\alpha3\beta2$ receptors (in $\alpha5\beta4$ KO)			
DMPP ($n = 8$)	10.97 ± 1.79	1.21 ± 0.12	39.29 ± 7.50‡
Cytisine ($n = 8$)	n.d.	n.d.	10.76 ± 1.59%§
Nicotine ($n = 11$)	22.51 ± 1.18	1.78 ± 0.18	36.20 ± 8.89‡
ACh ($n = 10$)	168.73 ± 25.20	0.67 ± 0.04	34.29 ± 5.81‡

The table shows the data of averaged fit parameters from dose–response curves of individual cells (n = number of cells): (A) $\alpha3\beta4$ receptors (see Fig. 6 for original current traces); (B) $\alpha3\beta4\alpha5$ receptors – SCG neurons of $\beta2$ KO mice contain about 60% $\alpha3\beta4$ and 40% $\alpha3\beta4\alpha5$ receptors (see Fig. 2B); (C) $\alpha3\beta2$ receptors (see Fig. 5 for original current traces). *Agonists not significantly different: one-way ANOVA ($F = 1.742$, $P = 0.1636$), followed by Newman–Keuls multiple comparison test (each comparison with a $P > 0.05$). †Agonists significantly different ($P = 0.0059$, Student's t-test). ‡Agonists not significantly different: one-way ANOVA ($F = 0.09781$, $P = 0.3429$), followed by Newman–Keuls multiple comparison test (each comparison with a $P > 0.05$). §Cytisine at saturating concentrations produced only 10.76 ± 1.59% of the effect of DMPP at $\alpha3\beta2$ receptors ($n = 8$). DMPP, 1-dimethyl-4-phenylpiperazinium iodide; n.d., not done.

TABLE 2. Decay of macroscopic currents differs significantly between $\alpha3\beta4$ and $\alpha3\beta2$, but not between $\alpha3\beta4$ and $\alpha3\beta4\alpha5$ nAChRs

	$\alpha3\beta4$ (n = 18)	$\alpha3\beta4\alpha5$ (n = 18)	P-value*	$\alpha3\beta2$ (n = 35)
Current amplitudes				
Af (%)†	13.0 ± 0.7	16.8 ± 1.1	0.0373	50.5 ± 2.1
As (%)	56.3 ± 2.3	48.6 ± 2.6	0.0119	36.2 ± 1.7
C (%)	30.5 ± 2.8	34.5 ± 2.8	0.3323	13.2 ± 1.0
Af + As + C (pA)	3747 ± 215	3907 ± 230	0.6174	1166 ± 77
Decay time constants				
τf (ms)	444 ± 22	449 ± 30	0.8922	132 ± 8
τs (ms)	5495 ± 496	5592 ± 509	0.8887	1129 ± 89
Capacitance (pF)	49.1 ± 2.3	57.7 ± 3.6	0.0567	54.1 ± 2.7

The decay of currents in response to 300 μM ACh (in the presence of 0.1 μM atropine) were fit to the sum of two exponential functions (see examples in Figs 5D and 6C) with two time constants τ_f (fast) and τ_s (slow) and three amplitudes: A_f (fast), A_s (slow) and a plateau C. †% of (Af + As + C) Note that time constants do not differ significantly between $\alpha3\beta4$ and $\alpha3\beta4\alpha5$ receptors (in SCG neurons taken from $\alpha5\beta2$ and $\beta2$ KO mice, respectively), whereas the relative contribution of A_f and A_s to the overall current differ slightly between the two genotypes ($P < 0.05$). In contrast, all parameters except for cell capacitance ($P = 0.2480$, Student's t-test) differ significantly between $\alpha3\beta4$ and $\alpha3\beta2$ receptors ($P < 0.01$, Student's t-test). *Student's t-test, comparing $\alpha3\beta4$ and $\alpha3\beta4\alpha5$.

effects were clearly less than in HEK tsA201 cells expressing $\alpha3\beta2$ (Wang *et al.*, 1998). Nonetheless, we routinely added nicotine to a final concentration of 100 μM after 1 day *in vitro* to our cultures and removed it at least 2 h before the recordings.

The most conspicuous, although not unexpected, feature of $\alpha3\beta2$ receptors is the rapid decline of macroscopic currents in response to nAChR agonists (Fig. 5A and D), consistent with rapid equilibration of activation and desensitization, favoring the desensitized state of this receptor subtype. When fitted to a double-exponential function, currents induced by 300 μM ACh decay with two time constants of 132 ± 8 (fast, τ_f) and 1129 ± 89 ms (slow, τ_s), respectively (Fig. 5D, Table 2). The rate of fluid exchange of our superfusion system (see Methods) is not fast enough for an accurate determination of concentration–response parameters of such rapidly desensitizing receptors and will cause an underestimation of the slope and of peak currents at high agonist concentrations. Relatively slowly desensitizing receptors such as $\alpha3\beta4$ will be less affected.

Notwithstanding this limitation, we can estimate EC_{50} values (Table 1) and thus rank the potencies of agonists for $\alpha3\beta2$ receptors. Given the low efficacy of cytisine at $\alpha3\beta2$ receptors [about 10% of the maximal currents of 1,1-dimethyl-4-phenylpiperazinium iodide (DMPP); Table 1, Fig. 5B] we did not construct dose–response curves

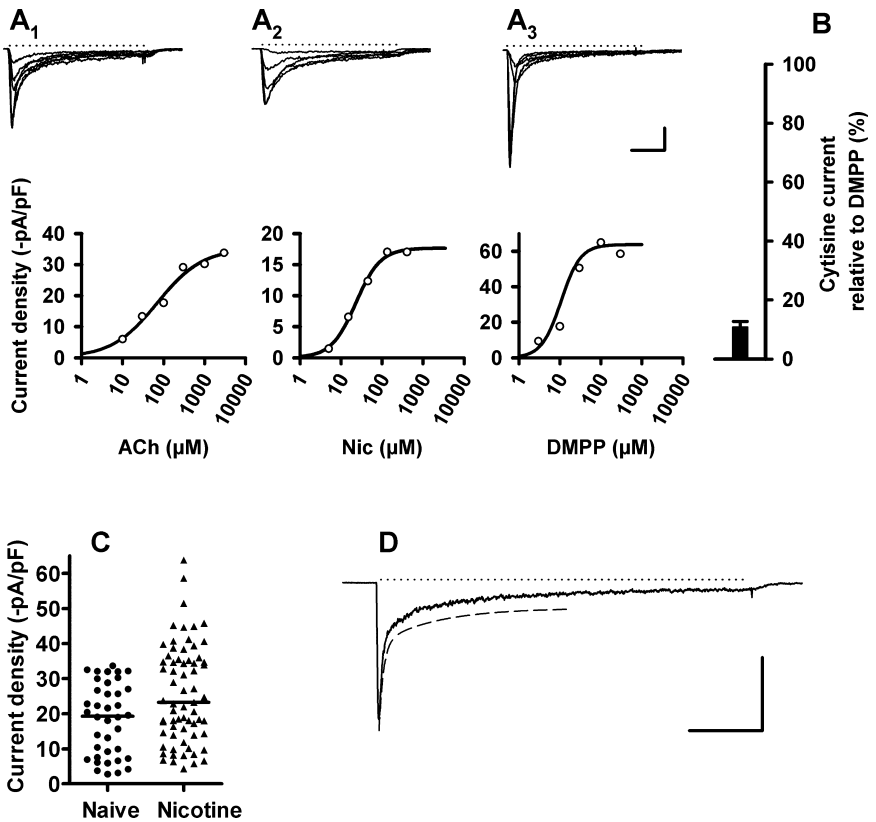

FIG. 5. Functional properties of $\alpha3\beta2$ nAChRs (analysed in $\alpha5\beta4$ KO mice). (A1–3) Agonist-induced currents (upper panels; applications indicated by dotted lines), and corresponding concentration–response curves (lower panels) by the nAChR agonists ACh (A1, in the presence of 0.1 μM atropine), nicotine (A2) and 1,1-dimethyl-4-phenylpiperazinium iodide (DMPP) (A3). In order to construct the dose–response curves, peak current amplitudes were fitted to the logistic equation shown in the Methods. Averaged fit parameters are provided in Table 1. Calibration A1–A3: 500 ms; 0.5 nA. (B) Low efficacy of cytisine at $\alpha3\beta2$ receptors: maxima taken from full DMPP dose–response curves were set in relation to responses by saturating concentrations of cytisine in the same cell. Cytisine at saturating concentrations produced only 10.76 ± 1.59% of the effect of DMPP (n = 8). (C) $\alpha3\beta2$ nAChR up-regulation by nicotine: peak currents in response to 300 μM ACh (in the presence of 0.1 μM atropine) in untreated cultures (Naïve; circles; n = 38), and in cultures treated for > 48 h with 100 μM nicotine (Nicotine; triangles; n = 67). Lines indicate median values of 19.3 and 23.2 pA/pF for naïve and nicotine-treated cultures, respectively; significantly different at $P = 0.0087$, Mann–Whitney test. (D) Rapid desensitization of $\alpha3\beta2$ nAChR. Patch clamp recording of an SCG neuron taken from a $\alpha5\beta4$ KO mouse, with current induced by 300 μM ACh (in the presence of 0.1 μM atropine, dotted line). Dashed line indicates decay of current fitted to the sum of two exponential functions (displaced for clarity from original trace by 200 pA). Fit parameters are 115 ms (τ_f, fast), 1477 ms (τ_s, slow), −1171 pA (A_f, fast), −472 pA (A_s, slow), −140 pA (plateau). Calibration: 2 s, 1 nA. Averaged fit parameters from identically designed experiments are provided in Table 2.

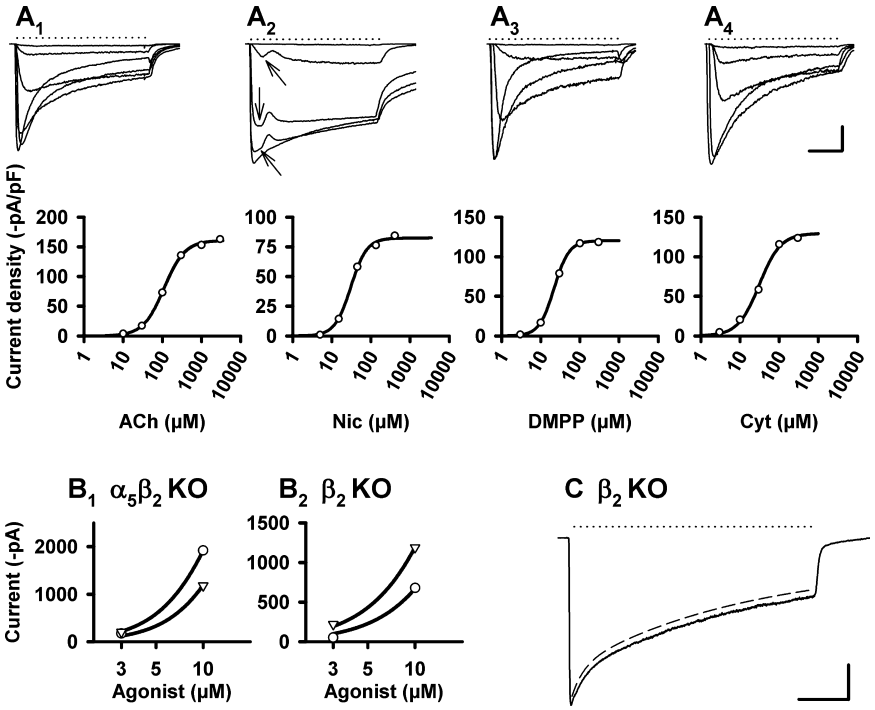

FIG. 6. Functional properties of $\alpha3\beta4$ nAChRs (in $\alpha5\beta2$ KO mice). (A) Agonist-induced currents (upper panels; applications indicated by dotted lines), and corresponding concentration–response curves (lower panels) by the nAChR agonists ACh (A1, in the presence of 0.1 μM atropine), nicotine (A2), DMPP (A3) and cytisine (A4). Arrows in A2 indicate an initial 'hump' discussed in the Results section. In order to construct the dose–response curves, peak current amplitudes were fitted to the logistic equation shown in the Methods. Averaged fit parameters are provided in Table 1. Calibration A1–A4: 500 ms; 2 nA. (B) Potency ratios determined from agonist-induced peak currents elicited at the low end of the concentration–response curves. (B1) $\alpha5\beta2$ KO: peak current amplitudes in response to 3 and 10 μM DMPP (circles) and cytisine (triangles), respectively, were fitted to the logistic equation with the constraints of a common slope and a maximum set to 7 nA. This resulted in fictitious EC_{50} values of 16.1 μM (DMPP) and 21.7 μM (cytisine) and a potency ration of 21.7/16.1 = 1.34. (B2) $\beta2$ KO: same protocol as described for B1. Fictitious EC_{50} values were 39.2 μM (DMPP) and 26.2 μM (cytisine), with a resulting potency ration of 0.67. Note that cytisine is more potent than DMPP in the $\beta2$ KO, whereas potencies are reversed in the $\alpha5\beta2$ double KO. Averaged potency ratios from identically designed experiments are provided in Fig. 7. (C) Patch clamp recording of an SCG neuron taken from a $\beta2$ KO mouse, with current induced by 300 μM ACh in the presence of 0.1 μM atropine (dotted line). Dashed line indicates decay of current fitted to the sum of two exponential functions (displaced for clarity from original trace by 200 pA). Fit parameters are 0.47 s (τ_f, fast), 6.98 s (τ_s, slow), −809 pA (A_f, fast), −2899 pA (A_s, slow), −943 pA (plateau). Calibration: 2 s, 1 nA. Averaged fit parameters from identically designed experiments are provided in Table 2.

for this substance, a known partial agonist/antagonist for receptors containing the $\beta2$ subunit (Luetje & Patrick, 1991; Papke & Heinemann, 1994; Nelson *et al.*, 2001). Because the $\alpha5$ subunit does not assemble into $\alpha3\beta2$ receptors (Figs 2D and 3A), we did not include the analysis of $\beta4$-single KO animals in our patch clamp experiments.

$\alpha3\beta4$ receptors in the mouse SCG

As documented above, about 55% of receptors in the SCG of WT animals consist of the subunits $\alpha3$ and $\beta4$, 24% also contain $\alpha5$, and 21% hold $\beta2$. Unlike in human IMR-32 cells, where $\alpha5$ (5%) and $\beta2$ (6%) contribute little to the overall number of $\alpha3\beta4$ receptors (Nelson *et al.*, 2001) we might thus expect more distinct differences in receptor function between WT and $\alpha5\beta2$ KO mice. Indeed, DMPP was more potent than cytisine in the SCG of $\alpha5\beta2$ KO mice (Table 1, and see Fig. 7), whereas the potencies of the two agonists are reversed in WT animals (Fischer *et al.*, 2005). This shift of agonist potencies seems primarily to be due to the deletion of the $\alpha5$ subunit, as we observed it as well in $\alpha5$-single KO mice (Fischer *et al.*, 2005). Although deletions of the subunits $\alpha5$ and $\beta2$ leave just $\alpha3\beta4$ receptors in the SCG we noticed two current components when using nicotine as an agonist (apparent as an early 'hump' in the current traces at lower concentrations, Fig. $6A_2$). One explanation of the phenomenon could be the presence of two receptors with an alternate stoichiometry. It has previously been shown that HEK 293 cells permanently transfected with the $\alpha4$ and the $\beta2$ subunits express both $2(\alpha4)3(\beta2)$ and $3(\alpha4)2(\beta2)$ receptors with different sensitivities to nAChR agonists, in particular ACh (Nelson *et al.*, 2003). By testing the hypothesis that $\alpha3\beta4$ receptors, expressed with varied stoichiometry in *Xenopus* oocytes, might also display different pharmacological properties, we found decreased potencies of both ACh and nicotine upon enhancing the presence of $\alpha3$ at the expense of $\beta4$ (supporting Fig. S3). When applied to our observations in the SCG, the first and the second peak could thus be due to the activation of $2(\alpha3)3(\beta4)$ and $3(\alpha3)2(\beta4)$, respectively. It is worth noting that $\alpha3$ mRNA exceed $\beta4$ levels by about a factor of 2 in the adult mouse SCG (Putz *et al.*, 2008).

$\alpha3\beta4\alpha5$ receptors in the mouse SCG

Deletion of the $\beta2$ subunit will leave $\alpha3\beta4\alpha5$ receptors, in addition to the more numerous $\alpha3\beta4$ subunit combination (Fig. 2C). Contrary to $\alpha5\beta2$ KO animals, cytisine was more potent than DMPP when the two agonists were used in low concentrations (Fig. 7: potency ratio 0.76 ± 0.04; significantly different from $\alpha5\beta2$ KO: $P < 0.001$, Newman–Keuls multiple comparison test following one-way ANOVA, $F = 28.47$, $P < 0.0001$; see also Fig. 6B). Low-concentration potency ratios were originally introduced to take differences of receptor desensitization at high agonist concentrations into account (Luetje & Patrick, 1991; Covernton *et al.*, 1994). In fact, the potency ratio of

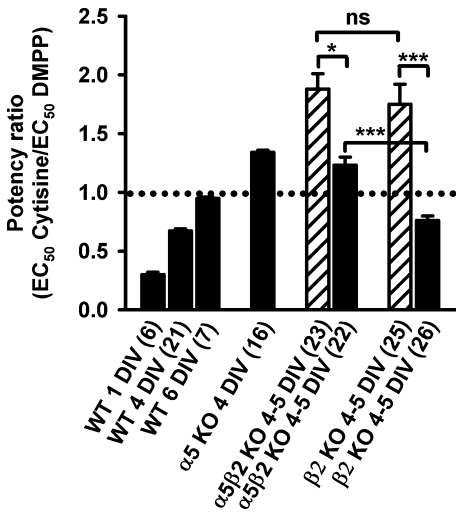

FIG. 7. Genotypes differ by their cytisine to DMPP potency ratios. Filled bars show mean ± SEM low-concentration potency ratios; hatched bars are mean ± SEM potency ratios deduced from full concentration–response curves of genotypes indicated at the abscissa. Potency ratios of cytisine by DMPP were calculated for individual cells by dividing the corresponding fictitious EC_{50} values (low concentration, see Fig. 6B for an example) or fully explored EC_{50} values (full concentration–response). Figures in parentheses are the number of cells. The data for WT and α5 KO are from Fischer *et al.* (2005). Ratios > 1 (above the dotted line) indicate a higher potency of DMPP. One-way ANOVA ($F = 28.47$, $P < 0.0001$), followed by Newman–Keuls multiple comparison test. n.s., not significantly different ($P > 0.05$); *significantly different ($P < 0.05$); ***significantly different ($P < 0.001$).

cytisine relative to DMPP calculated from responses at the lower end of the concentration–response curves differed significantly from results derived from full concentration–response curves for both genotypes (Fig. 7: one-way ANOVA, $F = 28.47$, $P < 0.0001$, followed by Newman–Keuls multiple comparison test: β2 KO: $P < 0.001$; α5β2 KO: $P < 0.05$ KO). Potency ratios of cytisine relative to DMPP at low concentrations have previously been shown to be sensitive discriminators for receptors containing the subunits α3 and β4 (Fischer *et al.*, 2005).

α3β4α5 expressed in *Xenopus* oocytes differ from α3β4 receptors by macroscopic currents with significantly faster decay time constants (Gerzanich *et al.*, 1998). We tested whether we could see such a difference in the decay of macroscopic currents between β2 KO (leaving α3α5β4 in addition to α3β4 receptors) and α5β2 KO (leaving just α3β4 receptors). However, when fitting the decay of current in response to 300 μM ACh to the sum of two exponential functions we found both the fast (τ_f) and the slow time constants (τ_s) unaffected by the presence of ACh. Nonetheless, the amplitude of the slow component increased slightly at the expense of the fast component when α5 was absent (Table 2).

Effects of the α-conotoxins AuIB and MII

Our double KO mice enabled us to investigate the effects of the two α-conotoxins AuIB and MII on 'pure' α3β4 and α3β2 receptors in SCG neurons and to compare these results with observations in WT animals (Fig. 8). α-Conotoxin AuIB rapidly and reversibly inhibited α3β4 receptors (Fig. $8A_2$ and A_3), with about one order of potency less than rat α3β4 receptors expressed in *Xenopus* oocytes (Luo *et al.*, 1998). In comparison with nAChRs in WT SCG (Fig. $8B_2$ and B_3), the currents induced by 300 μM ACh were somewhat more reduced in the α5β2 KO mice (Fig. $8B_3$: AuIB at 5 μM: α5β2 KO: 55.2 ± 2.9% of control, $n = 8$ cells; WT: 63 ± 2.4%, $n = 14$ cells; $P = 0.0483$, Student's *t*-test; AuIB at 10 μM: α5β2 KO: 34.0 ± 2.5%, $n = 7$ cells; WT: 43.0 ± 3.0%, $n = 8$ cells; $P = 0.0414$, Student's *t*-test), suggesting that co-assembling of the subunits α5 and/or β2 into α3β4 nAChRs interferes with the effect of the toxin. α-Conotoxin AuIB at 5 μM did not affect the currents induced in SCG neurons of α5β4 KO mice (Fig. $8C_1$).

α-Conotoxin MII, by contrast, rapidly inhibited α3β2 receptors with high potency (Fig. $8C_2$). Consistent with previous observations (Cartier *et al.*, 1996), recovery from inhibition was slow and incomplete (Fig. $8C_3$). α-Conotoxin MII at 100 nM did not affect α3β4 nAChRs (Fig. $8A_1$), but slightly reduced currents in response to 300 μM ACh in SCG neurons taken from WT animals (to 98.2% of control peak currents after 250 s of toxin application, $P = 0.0498$, one-sample Student's *t*-test with reference to a hypothetical 100%, $n = 13$ cells, Fig. $8B_1$). These observations are consistent with the reported high affinity and selectivity of α-conotoxin MII for α3β2 receptors (Cartier *et al.*, 1996) and suggest that few, if any, β2 subunits form an interface with α3 in WT SCG neurons. Importantly, we did not encounter SCG neurons of WT mice with currents that were particularly sensitive to the toxin. This is in contrast to α3-containing receptors in chick ciliary ganglion neurons that are highly susceptible to 300 nM α-conotoxin MII (Nai *et al.*, 2003).

Transganglionic neurotransmission in WT, α5β2 KO and α5β4 KO animals

We measured postganglionic compound action potentials of ganglia dissected from WT, α5β2 KO and α5β4 KO animals and found no significant differences in the amplitudes of the three preparations (Fig. 9). The experiments indicate that supramaximal stimulation of the preganglionic nerve will activate the same number of postganglionic nerves in the three genotypes. Hence, synaptic transmission is maintained despite a significantly reduced overall number of nAChRs in the α5β4 KO animals.

Discussion

With self-generated, subunit-specific antibodies we have established three types of hetero-pentameric receptors in the WT mouse SCG: α3β4 (55%), α3β4α5 (24%) and α3β4β2 (21%). Hence, all receptors in the SCG contain α3 and β4, and the subunits α5 and β2 are never co-assembled into the same receptor. Furthermore, targeted deletion of β4 also removed all α5-containing receptors, indicating that even under these stringent conditions, the α5 subunit could not be forced into assembly with β2. β4-Single KO mice – just as with α5β4-double KO – thus express only α3β2 hetero-pentameric receptors.

Mice lacking the β4 subunit had significantly reduced [^{3}H]-epibatidine binding and whole-cell currents, indicating less overall and cytoplasmic membrane nAChRs in this genotype. Nonetheless, the amplitude of compound action potentials recorded from postganglionic nerves did not differ significantly from WT animals.

Choline, a proposed α7-specific agonist, induced sizeable currents in SCG neurons from both α5β2-double and α5β2α7-triple KO mice, indicating that these currents are due to the activation of α3β4 receptors. In keeping with this conclusion, the currents in response to choline were negligible in α5β4-double KO animals. However, choline in the presence of the positive α7-specific modulator PNU-120596 induced currents (of variable amplitudes) in the α5β4-double KO and enhanced the currents in SCG neurons of α5β2-double KO mice.

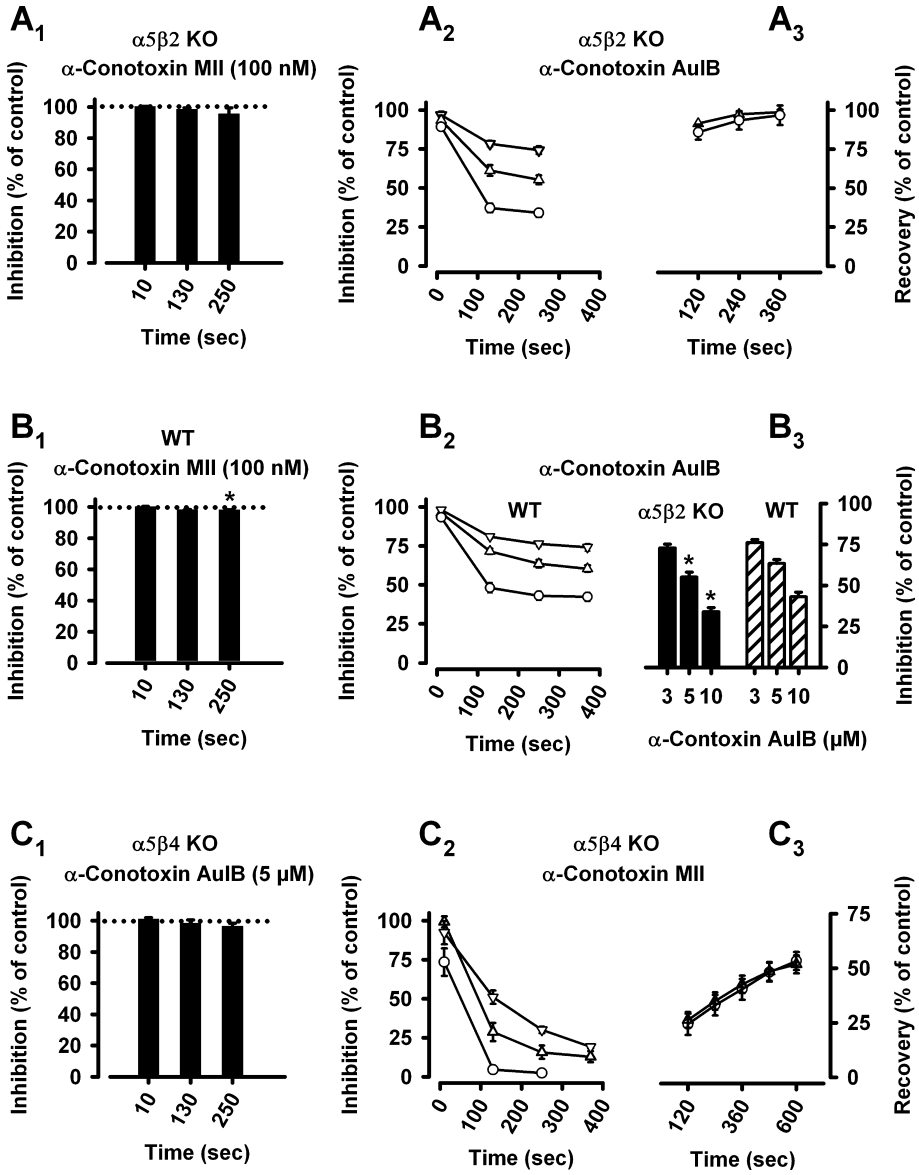

FIG. 8. Effects of the α-conotoxins AuIB and MII. Currents were induced by 300 μM ACh (in the presence of 0.1 μM atropine, 0.5 μM TTX and 0.1 mg/mL bovine serum albumin) in cultured SCG neurons of α5β2 KO (A1–A3, B3), WT (B1–B3) or α5β4 KO (C1–C3) mice, and in the absence (control, 100%) or presence of the α-conotoxins AuIB or MII. (A1) α5β2 KO mice: bars (mean percentage of currents relative to controls ± SEM, n = 7–9 cells) show the absence of effects of α-conotoxin MII on nAChRs in SCG neurons of α5β2 KO mice. The application of 100 nM α-conotoxin MII for indicated periods of time does not significantly decrease peak currents (one-sample Student's t-test with reference to a hypothetical 100%: $P_{10\ sec}$ = 0.6752; $P_{130\ sec}$ = 0.2009; $P_{250\ sec}$ = 0.3046). (A2) Time- and concentration-dependent inhibition by α-conotoxin AuIB of nAChRs remaining in SCG neurons of α5β2 KO mice. Down triangles: 3 μM (n = 5 cells); up triangles: 5 μM (n = 8 cells); circles: 10 μM α-conotoxin AuIB (n = 7 cells). Data points are the mean percentages of currents relative to controls ±SEM (shown if error bars exceed symbols). (A3) Fast and full recovery of the inhibition by 5 μM (down triangles, n = 3 cells) and 10 μM α-conotoxin AuIB (circles, n = 4 cells). (B1) WT mice: bars (mean percentage of currents relative to controls ± SEM, n = 13 cells) show little effect of α-conotoxin MII on nAChRs in SCG neurons of WT mice. The application of 100 nM α-conotoxin MII for indicated periods of time leaves 100.4% (after 10 s, P = 0.6119), 98.4% (after 130 s, P = 0.0534) and 98.2% (after 250 s, *P = 0.0498) of control peak currents (one-sample Student's t-test with reference to a hypothetical 100%). (B2) Time- and concentration-dependent inhibition by α-conotoxin AuIB of nAChRs in SCG neurons of WT mice. Down triangles: 3 μM (n = 8–11 cells); up triangles: 5 μM (n = 13–14 cells); circles: 10 μM α-conotoxin AuIB (n = 8 cells). Data points are the mean percentages of currents relative to controls ± SEM (shown if error bars exceed symbols). (B3) Concentration-dependent inhibition by indicated concentrations of conotoxin AuIB of nAChR currents in SCG neurons of α5β2 KO (filled bars) or WT (hatched bars) mice. Currents induced by 300 μM ACh were measured 250 s after toxin application and set in relation to control peak currents. AuIB has a significantly larger effect in α5β2 KO than in WT mice (AuIB at 5 μM: α5β2 KO: 55.2 ± 2.9%, n = 8 cells; WT: 63 ± 2.4%, n = 14 cells; *P = 0.0483, Student's t-test; AuIB at 10 μM: α5β2 KO: 34.0 ± 2.5%, n = 7 cells; WT: 43.0 ± 3.0%, n = 8 cells; *P = 0.0414, Student's t-test). (C1) α5β4 KO mice: bars (mean percentage of currents relative to controls ± SEM, n = 8 cells) show the absence of effects of α-conotoxin AuIB on nAChRs in SCG neurons of α5β4 KO mice. The application of 5 μM α-conotoxin AuIB for indicated periods of time does not significantly inhibit peak currents (one-sample Student's t-test with reference to a hypothetical 100%: $P_{10\ sec}$ = 0.1173; $P_{130\ sec}$ = 0.5057; $P_{250\ sec}$ = 0.0935). (C2) Time- and concentration-dependent inhibition by α-conotoxin MII of nAChRs remaining in SCG neurons of α5β4 KO mice. Down triangles: 10 nM (n = 8 cells); up triangles: 30 nM (n = 11 cells); circles: 100 nM α-conotoxin MII (n = 6 cells). Data points are the mean percentages of currents relative to controls ± SEM (shown if error bars exceed symbols). Note that 130 s exposure to 100 nM α-conotoxin MII blocks 95% of the currents. (C3) Slow and partial recovery of the inhibition by 30 nM (up triangles, n = 9 cells) and 100 nM α-conotoxin MII (circles, n = 6 cells).

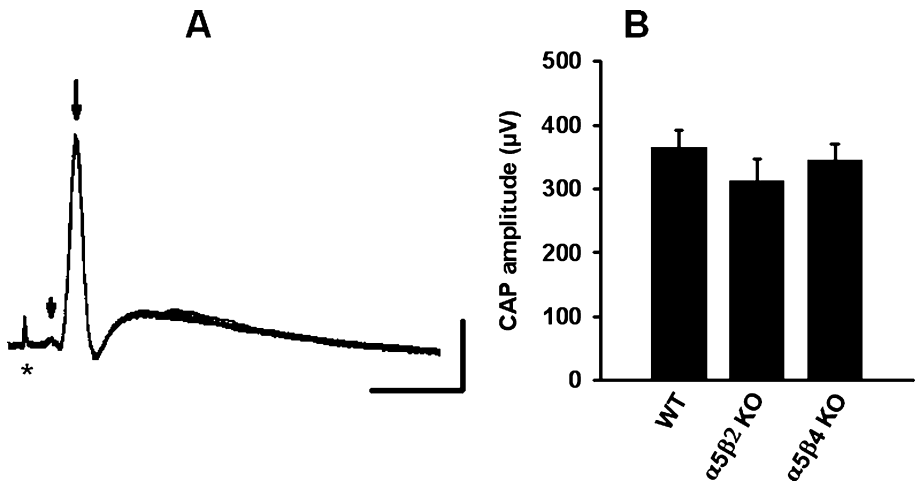

FIG. 9. Compound action potentials do not differ between genotypes. (A) Postganglionic compound action potentials (20 superimposed traces) recorded from the postganglionic (internal carotid) nerve in response to suprathreshold stimuli at 0.5 Hz to the preganglionic (SCG) nerve. Arrow shows the compound action potential, arrowhead the preganglionic potential and asterisk (*) the stimulation artifact. The ganglion was taken from a 5-week-old WT animal. Calibration: 20 ms, 200 μV. (B) Bars show mean ± SEM compound action potential amplitudes measured in SCGs taken from 4- to 6-week-old WT (n = 20), $\alpha5\beta2$ KO (n = 14) and $\alpha5\beta4$ KO (n = 16) mice. Note that mean amplitudes of either $\alpha5\beta2$ KO or $\alpha5\beta4$ do not differ significantly from WT [$P > 0.05$, one-way ANOVA ($F = 0.8223$, $P = 0.4457$), followed by a Dunnett's multiple comparison test with data referenced to WT].

'Pure' $\alpha3\beta4$ nAChRs were activated by the nicotinic receptor agonists with a rank order of potency DMPP > nicotine = cytisine > ACh. This rank order was similar for $\alpha3\beta2$ receptors, although cytisine was a poor agonist in the $\alpha5\beta4$ KO mice. Furthermore, $\alpha3\beta4$ and $\alpha3\beta2$ receptors differed remarkably in the decay of macroscopic currents and their responses to the α-conotoxins AuIB and MII. In contrast with previous observations in *Xenopus* oocytes (Wang *et al.*, 1996; Gerzanich *et al.*, 1998), we did not see an effect of the α5 subunit on the decay of macroscopic currents after $\alpha3\beta4$ receptor activation.

nAChRs in the rodent SCG

We found $\alpha3\beta4$, $\alpha3\beta4\beta2$ and $\alpha3\beta4\alpha5$ nAChRs in the mouse SCG, virtually identical to that in the rat based on their subunit composition, frequency of their occurrence and overall [^{3}H]-epibatidine binding (480 fmol/mg protein, Mao *et al.*, 2006). Likewise, the K_D of [^{3}H]-epibatidine binding in our membrane preparation (150.7 ± 25.6 pmol/L) compares well with previous findings in the adult (intact) mouse SCG (137 pmol/L, Del Signore *et al.*, 2002). This close similarity between the two species is noteworthy, as we have previously observed major differences of nAChR function at noradrenergic nerve terminals in the rat and mouse hippocampus (Scholze *et al.*, 2007).

nAChRs remaining after deletions of distinct subunits

In the brain, $\beta2$-containing receptors greatly outnumber receptors that contain $\beta4$ (McGehee & Role, 1995; Albuquerque *et al.*, 2009), and in most brain regions, targeted deletion of the $\beta2$ subunit virtually abolishes [^{3}H]-epibatidine binding and receptor autoradiography (Zoli *et al.*, 1998) due to the absence of a β subunit required to form functional nAChRs (Champtiaux & Changeux, 2004). Although both β subunits are expressed in the WT mouse SCG, we find the overall number of receptors in the $\beta4$ KO to be reduced by > 85% (to about the expression level of $\beta2$ in WT mice), indicating that $\beta2$ does not substitute for an absent $\beta4$ subunit. These results significantly extend our previous observation that $\beta2$ expression is tightly regulated (Putz *et al.*, 2008) and thus limits the formation of receptors in the SCG. Interestingly, the deletion of $\beta4$ also removed all receptors containing the α5 subunit, implying that α5 under no circumstances could be forced into co-assembling with $\alpha3\beta2$ in the mouse SCG. $\alpha3\beta2\alpha5$ have been expressed in *Xenopus* oocytes (Wang *et al.*, 1996; Gerzanich *et al.*, 1998) and in HEK293 cells (Nelson *et al.*, 2001), and may occur in the rat superior colliculus (see Gotti *et al.*, 2006). In contrast to $\beta4$-single and the $\alpha5\beta4$-double KO, deletions of either α5 or $\beta2$ had no effect on the overall number of receptors. Furthermore, the two subunits did not substitute for each other when one was deleted.

Functional characterization of hetero-pentameric nAChRs in the mouse SCG – lessons from KO mice

We and many others have used nAChR agonists for a 'pharmacological fingerprinting' of receptors (e.g. Colquhoun & Patrick, 1997b; Kristufek *et al.*, 1999; Fischer *et al.*, 2005; Gotti *et al.*, 2006). Our current patch clamp experiments show that DMPP activates somatic $\alpha3\beta4$ receptors (in the SCG of $\alpha5\beta2$-double KO mice) somewhat more potently than cytisine (low-concentration potency ratio of cytisine/DMPP: 1.23, Figs 6B$_1$ and 7). These data compare well with r$\alpha3\beta4$ receptors expressed in HEK cells (potency ratio: 1.47, Wong *et al.*, 1995) and human $\alpha3\beta4$ receptors in *Xenopus* oocytes (potency ratio: 4, Chavez-Noriega *et al.*, 1997) or HEK cells (potency ratio: 1.29, Nelson *et al.*, 2001). Other reports show cytisine to be more potent than DMPP for r$\alpha3\beta4$ receptors expressed in *Xenopus* oocytes (Luetje & Patrick, 1991; Covernton *et al.*, 1994) or in L-929 fibroblasts (Lewis *et al.*, 1997).

Removal of just the $\beta2$ subunit leaves $\alpha3\beta4$ receptors in the SCG with and without α5 that are overall more sensitive to cytisine than to DMPP (low-concentration potency ratio cytisine/DMPP: 0.76, Figs 6B$_2$ and 7). An increased potency of cytisine has previously been observed when α5 co-assembled with h$\alpha3\beta4$ receptors in *Xenopus* oocytes (Gerzanich *et al.*, 1998). We can, however, not confirm that the presence of α5 confers enhanced desensitization as well as increased calcium permeability to $\alpha3\beta4$ receptors also reported

in this study. We thus found no difference in the decay time constants of macroscopic currents between β2-single (leaving α3β4 and α3β4α5 receptors) and α5β2-double KO mice (leaving α3β4 receptors, this study), and enhanced calcium transients in response to nAChR activation in α5 KO compared with WT mice (Fischer *et al.*, 2005). In line with our observations, α5 had no effect on the decay time constants in HEK cells transfected with either hα3β4 (495 ms) or hα3α5β4 (563 ms, probed with 300 μM ACh, Nelson *et al.*, 2001).

α3β2 receptors investigated in α5β4-double KO mice distinctly differed from α3β4 receptors by a much faster decay of macroscopic currents and by a low efficacy of cytisine. These cardinal properties have consistently been observed when α3β2 receptors were heterologously expressed in *Xenopus* oocytes (e.g. Papke & Heinemann, 1994; Fenster *et al.*, 1997; Gerzanich *et al.*, 1998) or in HEK 293 cells (Wang *et al.*, 1998). However, data on the potency of agonists when tested on recombinant α3β2 receptors are less consistent by showing, for example, an exceptional low potency of nicotine (Covernton *et al.*, 1994) and a rather high potency of ACh (Luetje & Patrick, 1991). Our own results agree best with the observations in *Xenopus* oocytes by Gerzanich *et al.* (1998).

Types of nAChRs in the SCG of WT mice

The pharmacological profiles of nAChRs in our single and double KO models also help in resolving the functions of different nAChRs in the SCG of WT mice. As cytisine was consistently more potent than DMPP in every nerve cell of WT mice (Fischer *et al.*, 2005) we conclude that the α5 subunit is present in all neurons (absence of α5 reversed the cytisine/DMPP potency ratio, see Fischer *et al.*, 2005). The subtle influence of β2 on the effects of agonists (Colquhoun & Patrick, 1997a; Wang *et al.*, 2005) makes it more difficult to establish its impact on α3β4 nAChRs, and although we cannot exclude that α3β4β2 receptors are expressed just in a subset of neurons, our observations in β4 KO mice argue against a restricted expression of α3β4β2 nAChRs. In such a case we might expect neurons with α3β2 receptors as well as unresponsive cells without nAChRs (β4 deleted, β2 not present first hand), a phenomenon we did not observe. We furthermore did not encounter SCG neurons in WT mice with currents that were particularly sensitive to α-conotoxin MII and thus propose that all three types of receptors occur in all SCG neurons. In keeping with this conclusion, all neurons of the rat SCG showed immunoperoxidase staining with rabbit anti-α5 antibodies (Skok *et al.*, 1999).

Phenotype of mice with deletion of the β4 subunit

Our observation that amplitudes of compound action potentials recorded from postganglionic nerves do not differ between WT and α5β4 KO mice (Fig. 9) indicates that transganglionic neurotransmission is maintained in the SCG of KO animals. These observations are consistent with a previous report that bradycardia, induced by vagal nerve stimulation at 20 Hz, is not impaired in β4 KO mice (Wang *et al.*, 2003). Although α3β4* receptors are replaced by α3β2 (Fig. 2C), and although receptors are reduced to < 15% in the SCG of β4 KO mice (Fig. 1), the number of synaptic nAChRs appears to be sufficient to trigger action potentials in postsynaptic neurons upon preganglionic nerve activation. A previous observation that smooth muscle contractions of urinary bladder strips and of distal segments of the ileum, induced by bath-applied nAChR agonists, were significantly impaired in the β4 KO (Xu *et al.*, 1999b; Wang *et al.*, 2003) may be explained by the rapid desensitization of ganglionic α3β2 receptors (Fig. 5A and D) that remain in β4 KO mice (Fig. 2D). In contrast to less readily desensitizing α3β4 receptors, α3β2-mediated depolarization of parasympathetic ganglia in response to bath-applied agonists will be short-lasting, with fewer postganglionic nerve action potentials and therefore less transmitter release that cause smooth muscles to contract.

α3 is the only α subunit in the SCG that is able to form heteropentameric nAChRs, and deletion of α3 abolishes synaptic transmission in the SCG of mice (Xu *et al.*, 1999a; Rassadi *et al.*, 2005; Krishnaswamy & Cooper, 2009). Nonetheless, mice lacking α3 are vital and breed even in the absence of functional ganglionic nAChRs (Krishnaswamy & Cooper, 2009). What is important to note is these experiments done in laboratory conditions do not take into account the pressure of survival outside. In humans, both hyper- and under-activity of the autonomic nervous system may cause serious diseases (Xu *et al.*, 1999a; De Biasi, 2002; Lindstrom, 2002; Alkadhi *et al.*, 2005b; Wang *et al.*, 2007).

In our work we have addressed key issues on nAChR composition and function in the mouse sympathetic nervous system by a combined approach of immunoprecipitation, electrophysiology and deletions of distinct nAChR subunit genes. We show that transganglionic neurotransmission is maintained in our β4 mouse KO models despite significantly reduced levels of nAChRs. Our report confirms some but not all observations previously made on recombinant α3β4 and α3β2 receptors, stressing the necessity of further such studies on receptors in their native environment.

Supporting Information

Additional supporting information may be found in the online version of this article:

Fig. S1. Confirmation of the subunit specificity of antibodies by recombinant and native nAChRs.

Fig. S2. Effect of PNU-120596 on the current induced by 10 mM choline in a freshly dissociated E14 chick ciliary ganglion neuron.

Fig. S3. The pharmacological properties of α3β4 receptors are affected by their stoichiometry.

Please note: As a service to our authors and readers, this journal provides supporting information supplied by the authors. Such materials are peer-reviewed and may be re-organized for online delivery, but are not copy-edited or typeset by Wiley-Blackwell. Technical support issues arising from supporting information (other than missing files) should be addressed to the authors.

Acknowledgements

Expert technical assistance was provided by Gabriele Koth and Karin Schwarz. This study was supported by the Austrian Science Fund, Project P19325-B09, the Medizinische - Wissenschaftliche Fonds des Bürgermeisters des Bundeshauptstadt Wien grant 08070 and NIH grants MH53631 and GM48677.

Abbreviations

ACh, acetylcholine; $B_{max,}$ maximum binding capacity; DMPP, 1,1-dimethyl-4-phenylpiperazinium iodide; $K_{D,}$ dissociation constant; KO, knockout; MLA, methyllycaconitine; nAChR, nicotinic acetylcholine receptor; P18, postnatal day 18; PBS, phosphate-buffered saline; SCG, superior cervical ganglion; WT, wild type.

References

Albuquerque, E.X., Pereira, E.F.R., Alkondon, M. & Rogers, S.W. (2009) Mammalian nicotinic acetylcholine receptors: from structure to function. *Physiol. Rev.*, **89**, 73–120.

Alkadhi, K.A., Alzoubi, K.H. & Aleisa, A.M. (2005a) Plasticity of synaptic transmission in autonomic ganglia. *Prog. Neurobiol.*, **75**, 83–108.

Alkadhi, K.A., Alzoubi, K.H., Aleisa, A.M., Tanner, F.L. & Nimer, A.S. (2005b) Psychosocial stress-induced hypertension results from in vivo expression of long-term potentiation in rat sympathetic ganglia. *Neurobiol. Dis.*, **20**, 849–857.

Brejc, K., van Dijk, W.J., Schuurmans, M., van der Oost, J., Smit, A.G. & Sixma, T.K. (2001) Crystal structure of an ACh-binding protein reveals the ligand-binding domain of nicotinic receptors. *Nature*, **411**, 269–276.

Cartier, G.E., Yoshikami, D., Gray, W.R., Luo, S., Olivera, B.M. & McIntosh, J.M. (1996) A new α-conotoxin which targets α3β2 nicotinic acetylcholine receptors. *J. Biol. Chem.*, **271**, 7522–7528.

Champtiaux, N. & Changeux, J.-P. (2004) Knockout and knockin mice to investigate the role of nicotinic receptors in the central nervous system. *Prog. Brain Res.*, **145**, 235–251.

Champtiaux, N., Gotti, C., Cordero-Erausquin, M., David, D.J., Przybylski, C., Lena, C., Clementi, F., Moretti, M., Rossi, F.M., Le Novere, N., McIntosh, J.M., Gardier, A.M. & Changeux, J.-P. (2003) Subunit composition of functional nicotinic receptors in dopaminergic neurons investigated with knock-out mice. *J. Neurosci.*, **23**, 7820–7829.

Chavez-Noriega, L.E., Crona, J.H., Washburn, M.S., Urrutia, A., Elliott, K.J. & Johnson, E.C. (1997) Pharmacological characterization of recombinant human neuronal nicotinic acetylcholine receptors hα2β2, hα2β4, hα3β2, hα3β4, hα4β2, hα4β4, and hα7 expressed in *Xenopus* oocytes. *J. Pharmacol. Exp. Ther.*, **280**, 346–356.

Colquhoun, L.M. & Patrick, J. (1997a) α3, β2, and β4 form heterotrimeric neuronal nicotinic acetylcholine receptors in *Xenopus* oocytes. *J. Neurochem.*, **69**, 2355–2362.

Colquhoun, L.M. & Patrick, J.W. (1997b) Pharmacology of neuronal nicotinic acetylcholine receptor subtypes. *Adv. Pharmacol.*, **39**, 191–220.

Corringer, P.-J., Le Novere, N. & Changeux, J.-P. (2000) Nicotinic receptors at the amino acid level. *Annu. Rev. Pharmacol. Toxicol.*, **40**, 431–458.

Covernton, P.J.O., Kojima, H., Sivilotti, L.G., Gibb, A.J. & Colquhoun, D. (1994) Comparison of neuronal nicotinic receptors in rat sympathetic neurones with subunit pairs expressed in *Xenopus* oocytes. *J. Physiol.*, **481**, 27–34.

Cuevas, J., Roth, A.L. & Berg, D.K. (2000) Two distinct classes of functional α7-containing nicotinic receptor on rat superior cervical ganglion neurons. *J. Physiol.*, **525**, 735–746.

De Biasi, M. (2002) Nicotinic mechanisms in the autonomic control of organ systems. *J. Neurobiol.*, **53**, 568–589.

De Koninck, P. & Cooper, E. (1995) Differential regulation of neuronal nicotinic ACh receptor subunit genes in cultured neonatal rat by sympathetic neurons: specific induction of α7 by membrane depolarization of a Ca^{2+}/calmodulin dependent pathway. *J. Neurosci.*, **15**, 7966–7978.

Del Signore, A., Gotti, C., De Stefano, M.E., Moretti, M. & Paggi, P. (2002) Dystrophin stabilizes α3- but not α7-containing nicotinic acetylcholine receptor subtypes at the postsynaptic apparatus in the mouse superior cervical ganglion. *Neurobiol. Dis.*, **10**, 54–66.

Fenster, C.P., Rains, M.F., Noerager, B., Quick, M.W. & Lester, R.A.J. (1997) Influence of subunit composition on desensitization of neuronal acetylcholine receptors at low concentrations of nicotine. *J. Neurosci.*, **17**, 5747–5759.

Fischer, H., Orr-Urtreger, A., Role, L.W. & Huck, S. (2005) Selective deletion of the α5 subunit differentially affects somatic–dendritic versus axonally targeted nicotinic ACh receptors in mouse. *J. Physiol.*, **563**, 119–137.

Gerzanich, V., Wang, F., Kuryatov, A. & Lindstrom, J. (1998) α5 Subunit alters desensitization, pharmacology, Ca^{++} permeability and Ca^{++} modulation of human neuronal α3 nicotinic receptors. *J. Pharmacol. Exp. Ther.*, **286**, 311–320.

Gotti, C., Zoli, M. & Clementi, F. (2006) Brain nicotinic acetylcholine receptors: native subtypes and their relevance. *Trends Pharmacol. Sci.*, **27**, 482–491.

Houghtling, R.A., Davila-Garcia, M.I. & Kellar, K.J. (1995) Characterization of (+/−)-(3H)epibatidine binding to nicotinic cholinergic receptors in rat and human brain. *Mol. Pharmacol.*, **48**, 280–287.

Hurst, R.S., Hajos, M., Raggenbass, M., Wall, T.M., Higdon, N.R., Lawson, J.A., Rutherford-Root, K.L., Berkenpas, M.B., Hoffmann, W.E., Piotrowski, D.W., Groppi, V.E., Allaman, G., Ogier, R., Bertrand, S., Bertrand, D. & Arneric, S.P. (2005) A novel positive allosteric modulator of the α7 neuronal nicotinic acetylcholine receptor: In vitro and in vivo characterization. *J. Neurosci.*, **25**, 4396–4405.

Kedmi, M., Beaudet, A.L. & Orr-Urtreger, A. (2004) Mice lacking neuronal acetylcholine receptor β4-subunit and mice lacking both α5- and β4-subunits are highly resistant to nicotine-induced seizures. *Physiol. Genomics*, **17**, 221–229.

Krishnaswamy, A. & Cooper, E. (2009) An activity-dependent retrograde signal induces the expression of the high-affinity choline transporter in cholinergic neurons. *Neuron*, **61**, 272–286.

Kristufek, D., Stocker, E., Boehm, S. & Huck, S. (1999) Somatic and prejunctional nicotinic receptors in cultured rat sympathetic neurones show different agonist profiles. *J. Physiol.*, **516**, 739–756.

Lewis, T.M., Harkness, P.C., Sivilotti, L.G., Colquhoun, D. & Millar, N.S. (1997) The ion channel properties of rat recombinant neuronal nicotinic receptor are dependent on the host cell type. *J. Physiol.*, **505**, 299–306.

Lindstrom, J. (2002) Autoimmune diseases involving nicotinic receptors. *J. Neurobiol.*, **53**, 656–665.

Luetje, C.W. & Patrick, J. (1991) Both α- and β-subunits contribute to the agonist sensitivity of neuronal nicotinic acetylcholine receptors. *J. Neurosci.*, **11**, 837–845.

Luo, S., Kulak, J.M., Cartier, G.E., Jacobsen, R.B., Yoshikami, D., Olivera, B.M. & McIntosh, J.M. (1998) α-Conotoxin AuIB selectively blocks α3β4 nicotinic acetylcholine receptors and nicotine-evoked norepinephrine release. *J. Neurosci.*, **18**, 8571–8579.

Mandelzys, A., De Koninck, P. & Cooper, E. (1995) Agonist and toxin sensitivities of ACh-evoked currents on neurons expressing multiple nicotinic receptor subunits. *J. Neurophysiol.*, **74**, 1212–1221.

Mao, D., Yasuda, R.P., Fan, H., Wolfe, B.B. & Kellar, K.J. (2006) Heterogeneity of nicotinic cholinergic receptors in rat superior cervical and nodosa ganglia. *Mol. Pharmacol.*, **70**, 1693–1699.

McGehee, D.S. & Role, L.W. (1995) Physiological diversity of nicotinic acetylcholine receptors expressed by vertebrate neurons. *Annu. Rev. Physiol.*, **57**, 521–546.

Millar, N.S. (2008) RIC-3: a nicotinic acetylcholine receptor chaperone. *Br. J. Pharmacol.*, **153**, S177–S183.

Moser, N., Mechawar, N., Jones, I., Gochberg-Sarver, A., Orr-Urtreger, A., Plomann, M., Salas, R., Molles, B., Marubio, L., Roth, U., Maskos, U., Winzer-Serhan, U., Bourgeois, J.P., Le Sourd, A.M., De Biasi, M., Schroder, H., Lindstrom, J., Maelicke, A., Changeux, J.P. & Wevers, A. (2007) Evaluating the suitability of nicotinic acetylcholine receptor antibodies for standard immunodetection procedures. *J. Neurochem.*, **102**, 479–492.

Nai, Q., McIntosh, J.M. & Margiotta, J.F. (2003) Relating neuronal nicotinic acetylcholine receptor subtypes defined by subunit composition and channel function. *Mol. Pharmacol.*, **63**, 311–324.

Nelson, M.E., Wang, F., Kuryatov, A., Choi, C.H., Gerzanich, V. & Lindstrom, J. (2001) Functional properties of human nicotinic AChRs expressed by IMR-32 neuroblastoma cells resemble those of α3β4 AChRs expressed in permanently transfected HEK cells. *J. Gen. Physiol.*, **118**, 563–582.

Nelson, M.E., Kuryatov, A., Choi, C.H., Zhou, Y. & Lindstrom, J. (2003) Alternate stoichiometries of α4β2 nicotinic acetylcholine receptors. *Mol. Pharmacol.*, **63**, 332–341.

Orr-Urtreger, A., Göldner, F.M., Saeki, M., Lorenzo, I., Goldberg, L., De Biasi, M., Dani, J.A., Patrick, J.W. & Beaudet, A.L. (1997) Mice deficient in the α7 neuronal nicotinic acetylcholine receptor lack α-bungarotoxin binding sites and hippocampal fast nicotinic currents. *J. Neurosci.*, **17**, 9165–9171.

Papke, R.L. & Heinemann, S.F. (1994) Partial agonist properties of cytisine on neuronal nicotinic receptors containing the β2 subunit. *Mol. Pharmacol.*, **45**, 142–149.

Papke, R.L., Bencherif, M. & Lippiello, P.M. (1996) An evaluation of neuronal nicotinic acetylcholine receptor activation by quaternary nitrogen compounds indicates that choline is selective for the α7 subtype. *Neurosci. Lett.*, **213**, 201–204.

Picciotto, M.R., Zoli, M., Lena, C., Bessis, A., Lallemand, Y., Le Novere, N., Vincent, P., Pich, E.M., Brulet, P. & Changeux, J.-P. (1995) Abnormal avoidance learning in mice lacking functional high-affinity nicotine receptor in the brain. *Nature*, **374**, 65–67.

Pollock, V.V., Pastoor, T., Katnik, C., Cuevas, J. & Wecker, L. (2009) Cyclic AMP-dependent protein kinase A and protein kinase C phosphorylate α4β2 nicotinic receptor subunits at distinct stages of receptor formation and maturation. *Neuroscience*, **158**, 1311–1325.

Putz, G., Kristufek, D., Orr-Urtreger, A., Changeux, J.P., Huck, S. & Scholze, P. (2008) Nicotinic acetylcholine receptor-subunit mRNAs in the mouse superior cervical ganglion are regulated by development but not by deletion of distinct subunit genes. *J. Neurosci. Res.*, **86**, 972–981.

Rae, J., Cooper, K., Gates, P. & Watsky, M. (1991) Low access resistance perforated patch recordings using amphotericin B. *J. Neurosci. Methods*, **37**, 15–26.

Rassadi, S., Krishnaswamy, A., Pie, B., McConnell, R., Jacob, M.H. & Cooper, E. (2005) A null mutation for the α3 nicotinic acetylcholine (ACh) receptor gene abolishes fast synaptic activity and reveals that ACh output from developing preganglionic terminals is regulated in an activity-dependent manner. *J. Neurosci.*, **25**, 8555–8566.

Scholze, P., Orr-Urtreger, A., Changeux, J.P., McIntosh, J.M. & Huck, S. (2007) Catecholamine outflow from mouse and rat brain slice preparations evoked by nicotinic acetylcholine receptor activation and electrical field stimulation. *Br. J. Pharmacol.*, **151**, 414–422.

Severance, E.G., Zhang, H., Cruz, Y., Pakhlevaniants, S., Hadley, S.H., Amin, J., Wecker, L., Reed, C. & Cuevas, J. (2004) The α7 nicotinic acetylcholine receptor subunit exists in two isoforms that contribute to functional ligand-gated ion channels. *Mol. Pharmacol.*, **66**, 420–429.

Sharples, C.G.V., Kaiser, S., Soliakov, L., Marks, M.J., Collins, A.C., Washburn, M., Wright, E., Spencer, J.A., Gallagher, T., Whiteaker, P. & Wonnacott, S. (2000) UB-165: a novel nicotinic agonist with subtype selectivity implicates the α4β2* subtype in the modulation of dopamine release from rat striatal synaptosomes. *J. Neurosci.*, **20**, 2783–2791.

Sivilotti, L.G., McNeil, D.K., Lewis, T.M., Nassar, M.A., Schoepfer, R. & Colquhoun, D. (1997) Recombinant nicotinic receptors, expressed in *Xenopus* oocytes, do not resemble native rat sympathetic ganglion receptors in single-channel behaviour. *J. Physiol.*, **500**, 123–138.

Skok, M.V., Voitenko, L.P., Voitenko, S.V., Lykhmus, E.Y., Kalashnik, E.N., Litvin, T.I., Tzartos, S.J. & Skok, V.I. (1999) Alpha subunit composition of nicotinic acetylcholine receptors in the rat autonomic ganglia neurons as determined with subunit-specific anti-α(181–192) peptide antibodies. *Neuroscience*, **93**, 1427–1436.

Wang, F., Gerzanich, V., Wells, G.B., Anand, R., Peng, X., Keyser, K. & Lindstrom, J. (1996) Assembly of human neuronal nicotinic receptor α5 Subunits with α3, β2, and β4 subunits. *J. Biol. Chem.*, **271**, 17656–17665.

Wang, F., Nelson, M.E., Kuryatov, A., Olale, F., Cooper, J., Keyser, K. & Lindstrom, J. (1998) Chronic nicotine treatment up-regulates human α3β2 but not α3β4 acetylcholine receptors stably transfected in human embryonic kidney cells. *J. Biol. Chem.*, **273**, 28721–28732.

Wang, N., Orr-Urtreger, A., Chapman, J., Rabinowitz, R., Nachmann, R. & Korczyn, A.D. (2002a) Autonomic function in mice lacking α5 neuronal nicotinic acetylcholine receptor subunit. *J. Physiol.*, **542**, 347–354.

Wang, N., Orr-Urtreger, A. & Korczyn, A.D. (2002b) The role of neuronal nicotinic acetylcholine receptor subunits in autonomic ganglia: lessons from knockout mice. *Prog. Neurobiol.*, **68**, 341–360.

Wang, N., Orr-Urtreger, A., Chapman, J., Rabinowitz, R. & Korczyn, A.D. (2003) Deficiency of nicotinic acetylcholine receptor β4 subunit causes autonomic cardiac and intestinal dysfunction. *Mol. Pharmacol.*, **63**, 574–580.

Wang, N., Orr-Urtreger, A., Chapman, J., Ergun, Y., Rabinowitz, R. & Korczyn, A.D. (2005) Hidden function of neuronal nicotinic acetylcholine receptor β2 subunits in ganglionic transmission: comparison to α5 and β4 subunits. *J. Neurol. Sci.*, **228**, 167–177.

Wang, Z., Low, P.A., Jordan, J., Freeman, R., Gibbons, C.H., Schroeder, C., Sandroni, P. & Vernino, S. (2007) Autoimmune autonomic ganglionopathy – IgG effects on ganglionic acetylcholine receptor current. *Neurology*, **68**, 1917–1921.

Wong, E.T., Holstad, S.G., Mennerick, S.J., Hong, S.E., Zorumski, C.F. & Isenberg, K.E. (1995) Pharmacological and physiological properties of a putative ganglionic nicotinic receptor, α3β4, expressed in transfected eucaryotic cells. *Mol. Brain Res.*, **28**, 101–109.

Xu, W., Gelber, S., Orr-Urtreger, A., Armstrong, D., Lewis, R.A., Ou, C.N., Patrick, J., Role, L., De Biasi, M. & Beaudet, A.L. (1999a) Megacystis, mydriasis, and ion channel defect in mice lacking the α3 neuronal nicotinic acetylcholine receptor. *Proc. Natl Acad. Sci. USA*, **96**, 5746–5751.

Xu, W., Orr-Urtreger, A., Nigro, F., Gelber, S., Sutcliffe, C.B., Armstrong, D., Patrick, J.W., Role, L.W., Beaudet, A.L. & De Biasi, M. (1999b) Multiorgan autonomic dysfunction in mice lacking the β2 and the β4 subunits of neuronal nicotinic acetylcholine receptors. *J. Neurosci.*, **19**, 9298–9305.

Zhang, Z., Vijayaraghavan, S. & Berg, D.K. (1994) Neuronal acetylcholine receptors that bind α-bungarotoxin with high affinity function as ligand-gated ion channels. *Neuron*, **12**, 167–177.

Zoli, M., Lena, C., Picciotto, M.R. & Changeux, J.-P. (1998) Identification of four classes of brain nicotinic receptors using β2 mutant mice. *J. Neurosci.*, **18**, 4461–4472.

Zwart, R. & Vijverberg, H.P.M. (1998) Four pharmacologically distinct subtypes of α4β2 nicotinic acetylcholine receptor expressed in *Xenopus laevis* oocytes. *Mol. Pharmacol.*, **54**, 1124–1131.